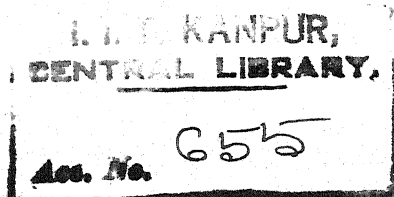


VIBRATIONAL STUDIES ON L-ALANINE AND POLY-L-ALANINE

A Thesis Submitted
In Partial Fulfilment of the Requirements
for the Degree of
DOCTOR OF PHILOSOPHY



by
M.V. KRISHNAN

POST GRADUATE OFFICE
This thesis has been approved
for the award of the Degree of
Doctor of Philosophy (Ph.D.)
in accordance with the
regulations of the Indian
Institute of Technology Kanpur
Dated: 15/11/70 *B*

TH
PHY/1970/D
K 897 v

to the
Department of Physics
INDIAN INSTITUTE OF TECHNOLOGY KANPUR

September 1970

Thesis
539.12
K 897

PHY - 1970 - D - KRI - VIR

CERTIFICATE

Certified that this work on "VIBRATIONAL STUDIES ON L-ALANINE AND POLY-L-ALANINE" by M.V. Krishnan has been carried out under my supervision and that this has not been submitted elsewhere for a degree.

V.D. Gupta
21/9/70

Dr. V.D. Gupta
Assistant Professor
Department of Physics
Indian Institute of Technology Kanpur

POST GRADUATE OFFICE
This thesis has been approved
for the award of the Degree of
Doctor of Philosophy (Ph.D.)
in accordance with the
regulations of the Indian
Institute of Technology Kanpur
Dated: 15/11/71 *R*

ACKNOWLEDGEMENTS

The author wishes to express his indebtedness to

. V.D. Gupta for suggesting the problem and for his kind encouragement and stimulating guidance throughout the course of this work.

The author is thankful to Professor J. Mahanty for his interest in the work.

The author is indebted to the scientists at the Army Materials and Mechanics Research Centre, U.S.A., for obtaining the neutron spectra of L-alanine and α -poly-L-alanine which have been reported in this work, and to Dr. T. Miyazawa of Osaka University, Japan, for information regarding the force field for β -polyalanine.

The facilities provided at the Computer Centre, IIT-Bombay are gratefully acknowledged.

The author wishes to thank Mr. M. Natsu for patient and careful typing of the thesis, and Mr. H.K. Panda for running the stencils.

The research was supported in part by a grant from the U.S. Department of Agriculture under P.L.-480, which is gratefully acknowledged.

TABLE OF CONTENTS

	<u>Page</u>
LIST OF TABLES	v
LIST OF FIGURES	vi
SYNOPSIS	vii
CHAPTER I - INTRODUCTION	1
CHAPTER II - GENERAL THEORY	9
2.1 Molecular vibrations of finite molecules	9
2.2 Molecular vibrations of polymer chains	11
2.3 The use of neutron scattering	21
CHAPTER III - LOW-FREQUENCY VIBRATION SPECTRA OF L-ALANINE	33
CHAPTER IV - THE α -HELICAL FORM OF POLY-L-ALANINE	44
CHAPTER V - THE β -FORM OF POLY-L-ALANINE	74
CHAPTER VI - CONCLUSION	95

LIST OF TABLES

	<u>Page</u>
1. OBSERVED INFRARED AND NEUTRON FREQUENCIES FOR L-ALANINE	40
2. COORDINATES OF ATOMS IN AN α -POLY-L-ALANINE RESIDUE	48
3. CHARACTER TABLE, NUMBERS OF NORMAL MODES AND THEIR OPTICAL ACTIVITY FOR THE C(10 π /18) FACTOR GROUP	49
4. G MATRIX ELEMENTS FOR α -POLY-L-ALANINE	53
5. FORCE CONSTANTS FOR α -POLY-L-ALANINE	58
6. F MATRIX ELEMENTS FOR α -POLY-L-ALANINE	59
7. CALCULATED AND OBSERVED FREQUENCIES FOR α -POLY-L-ALANINE	64
8. CHARACTER TABLE, NUMBERS OF NORMAL MODES AND THEIR OPTICAL ACTIVITY FOR THE C(π) FACTOR GROUP	76
9. G MATRIX ELEMENTS FOR β -POLY-L-ALANINE	79
10. FORCE CONSTANTS FOR β -POLY-L-ALANINE	82
11. F MATRIX ELEMENTS FOR β -POLY-L-ALANINE	83
12. CALCULATED AND OBSERVED FREQUENCIES FOR β -POLY-L-ALANINE	87

LIST OF FIGURES

	<u>Page</u>
1. SCHEMATIC OF A COLD NEUTRON FACILITY	24
2. INFRARED SPECTRUM OF L-ALANINE	34
3. INELASTIC NEUTRON SPECTRUM OF L-ALANINE	35
4. INFRARED SPECTRUM OF β -ALANINE	36
5. MOLECULE AND CRYSTAL STRUCTURE OF L-ALANINE	38
6. THE α -HELIX OF POLYALANINE	47
7. PORTION OF α -HELICAL STRUCTURE SHOWING INDICES OF THE ATOMS	51
8. INFRARED SPECTRUM OF α -POLY-L-ALANINE	61
9. DISPERSION CURVES AND FREQUENCY DISTRIBUTION FOR THE α -HELIX OF POLYALANINE	62
10. DISPERSION CURVES AND FREQUENCY DISTRIBUTION FOR POLYGLYCINE I	71
11. UNIT CELL OF POLYALANINE CHAIN IN THE β -FORM	77
12. a. INFRARED SPECTRUM OF β -POLYALANINE FROM 1800 - 700 cm^{-1}	85
b. INFRARED SPECTRUM OF β -POLYALANINE FROM 700 - 100 cm^{-1}	86
13. DISPERSION CURVES FOR β -POLYALANINE	91

SYNOPSIS

VIBRATIONAL STUDIES ON L-ALANINE AND POLY-L-ALANINE

M.V. Krishnan

Ph.D.

Department of Physics

Indian Institute of Technology Kanpur

September 1970

The thesis is concerned with a study of the vibrational properties of L-alanine and poly-L-alanine. Polyalanine is one of the simplest of the synthetic polypeptides, and exists in two forms differing in their chain conformation. In one form, the chain is in the well-known alpha-helical conformation, and is stabilised by intramolecular hydrogen bonds; in the other form, known as the beta-configuration, polyalanine exists as nearly fully-extended chains, arranged in antiparallel pleated sheets. Intermolecular N - H...O hydrogen bonds are formed between adjacent chains. Much of the work in the thesis is devoted to a treatment of the normal modes of vibration and their dispersion in the two forms of polyalanine.

The first chapter forms a general introduction to the thesis; the importance of conformation studies in polypeptides and proteins is described and some of the important methods for characterisation of conformations are briefly outlined. These techniques include optical rotatory dispersion, circular

ichroism and deuterium exchange measurements. Infrared absorption spectroscopy is an important tool in this connection, and one with which the thesis is more directly related. The usefulness of amide bands in conformation studies has been pointed out and the motivation for the present work has been expressed in terms of a need for gaining more information on the relation between conformation and the nature of normal modes and their dispersion, especially in the low-frequency region.

In Chapter II of the thesis the theoretical method used for the treatment of the normal vibrations of helical polymer chains is described. Higgs' modification of the well-known F-matrix method based on the use of the screw symmetry of helical molecules is discussed. The method of solution of the secular equations is also described. In addition to infrared techniques, inelastic neutron scattering is also a useful tool of molecular spectroscopy. The importance of neutron scattering techniques in studying vibrational properties of polymer systems is pointed out in this chapter and some of the relevant results of the theory of inelastic neutron scattering in connection with spectral analysis are outlined. In particular, the frequency distributions obtained from dispersion curve calculations would be of help in the analysis of neutron spectra.

Chapter III deals with a study of the low frequency vibrational spectra of L-alanine, the monomer from which the polyalanine chain is built. The infrared spectrum obtained in

the region below 700 cm^{-1} and the inelastic neutron spectrum have been made use of. Based on the fact that the intensities of neutron peaks are weighted by the amplitudes of motion of the protons, possible assignments of the peak positions are given and discussed.

The next two chapters form the central portion of the thesis. In the first of these the complete vibrational analysis of the alpha-helical chain of polyalanine based on Higgs' modification of the GF-matrix method is described. The potential energy distributions have been used in making assignments of optically active frequencies. Use has also been made of the inelastic neutron spectrum of polyalanine in this connection. The force field has been obtained and the dispersion curves have been plotted. From the dispersion curves, the frequency distribution has been derived and compared with that obtained from the inelastic neutron spectrum. The fifth chapter is an account of similar calculations on the beta-form of polyalanine. In these chapters several features of the dispersion curves are discussed and an attempt is made to analyse significant features of these curves in a comparative study in connection with the conformation. In this connection the dispersion curves for the low frequency torsional modes are compared with those for polyglycine I.

In Chapter VI, which forms the concluding portion of the thesis, the limitations of the above calculations are discussed in view of the fact that the polypeptide has been

regarded as an isolated single chain; the possibility of further calculations on three-dimensional systems is considered. The effect of intermolecular interactions on the vibrational properties and dispersion curves is outlined. Suggestions are made for further work, and the usefulness of dispersion curve calculations in understanding thermodynamic behaviour is discussed.

CHAPTER I

INTRODUCTION

As early as the beginning of the present century it was recognised that polypeptide chains are a major constituent of proteins. This fact endows the synthetic polypeptides and their basic monomers, the alpha-amino carboxylic acids with a particular interest, since the polypeptides may be regarded as simple models for a study of proteins. The synthetic polypeptides are also of interest as high polymers in their own right, apart from the specific interest due to their relationship to the proteins. Thus all naturally occurring fibres- wool, hair, the silks- are polypeptides, and high-molecular-weight synthetic materials like nylon, which are good fibre-formers, contain the peptide group.

One of the important characteristics of protein or polypeptide chains is the chain conformation. In this connection, it would be useful to describe the different levels at which the structure of proteins and large polypeptide molecules is discussed. The primary structure of a protein is concerned with the formation of covalent bonds and the numerical order or arrangement of amino acids in the chain, i.e., the amino acid sequence. The secondary and tertiary structures of a polypeptide describe its conformation. Secondary structure is the spatial relationship of neighbouring atoms along the chain. Tertiary structure is concerned

with the various shapes assumed by the polypeptide chain, in other words, it refers to gross folding of the chain, which may bring into proximity parts of the molecule otherwise widely separated along its backbone. The chemical, physical and biological properties of a protein are largely dictated by its conformation. When the conformation of a protein is altered from that of its native state, loss of specific biological function usually occurs; the protein is said to be denatured. Considerable interest is, therefore, attached to the determination and characterisation of chain conformations in proteins and polypeptides.

Several methods are used for studying the conformations of macromolecular chains. X-ray diffraction can specify with certainty the relative positions of atoms in an ordered molecule, and is hence capable of distinguishing between different conformations. X-ray diffraction has been successfully employed in elucidating the structures of several proteins and polypeptides¹. However, this type of detailed steric analysis must be carried out in the solid state, and focuses attention on only those parts of the polymer which are crystalline.

The fact that proteins and other biological molecules in their functional state exist in solution has led to the development of a number of techniques primarily concerned with studying conformations in solution. Helical molecules in solution can be discriminated by a combination of light scattering and hydrodynamic techniques, both of which yield

information on the shape and dimensions of macromolecules. Flow birefringence and the measurement of intrinsic viscosity have been used to study conformations in solution of several polypeptides².

Optical rotation has proved to be a useful tool for studying structural properties of optically active polypeptides in solution³⁻⁸. It is common practice to use rotatory power at one wavelength to detect structural alteration, as in the study of helix-coil transitions and denaturation, but monochromatic data often do not alone permit a distinct specification of the change that takes place. Optical rotatory dispersion (ORD), i.e., the variation of optical rotatory power with wavelength, can, in principle, provide a greater amount of information that may be correlated with structure and, therefore, offers a basis for more perceptive studies of conformation and conformational change. A related tool, which provides considerable information when used for conformational studies, is the measurement of circular dichroism (CD), the difference in absorption of left- and right-circularly polarised light^{7,9}.

High resolution NMR spectroscopy has found increasing application in the study of conformational changes in polypeptides. The first NMR study of the helix-coil transition was reported by Bovey et al¹⁰. NMR techniques have since then been used extensively to provide a sensitive measure of helical content for a number of polypeptides in solution¹¹.

The chemical shift behaviour of NMR peaks has provided some insight into the nature of helix-random coil transformations.

Measurements of the rates of hydrogen-deuterium exchange between a dissolved protein or polypeptide and a surrounding solvent have revealed a characteristic difference between the helical and random coil conformations. The method of deuterium exchange is thus useful for characterisation of conformations¹². Small-angle X-ray scattering has, in recent years, been used as an effective tool for studying conformations of polypeptides in solution¹³.

An important technique for the study of conformations of polypeptides, and one with which the work described in the following pages is more directly related, is infrared spectroscopy. Conformational analyses of polypeptides and proteins using infrared absorption spectra have largely been made in terms of the amide bands, which arise out of characteristic vibrational modes of the amide group. Ambrose and Elliott¹⁴ first found the correlations between the amide I and II bands and the chain conformation. Both the frequencies of these bands and their dichroism depend on the conformation. Further investigation established that the frequency criteria for distinguishing between conformations and the differences in dichroic behaviour held for synthetic polypeptides in solution as well as in the solid phase^{15,16}. Theoretical interpretations to these correlations were then given¹⁷. Accordingly the alpha-helical form, parallel-chain beta-form,

antiparallel-chain beta-form and disordered form have been distinguished by the amide I and II bands observed with oriented samples of polypeptides and fibrous proteins. However, because the alpha-helical form and the disordered form exhibit similar amide I and II bands, the usefulness of these correlations is somewhat limited for unoriented protein samples where a few types of conformations possibly coexist¹⁸. Infrared studies of polypeptides in the region below 800 cm^{-1} were thus made with a view to obtaining some additional correlations which would be useful for structure diagnoses. In fact, the amide V band, which arises out of the N - H out-of-plane bending mode, was found to be useful for conformation diagnoses¹⁹. Miyazawa and coworkers²⁰ studied the amide V bands for a series of polypeptides and concluded that the correlations between the frequencies of these bands and conformations are considerably more useful for conformation diagnoses, particularly for copolyamino-acids or proteins which are not oriented.

The vibrational modes giving rise to the amide I and II bands consist principally of the $\text{C}=\text{O}$ stretching and N-H in-plane bending and C-N stretching modes of the amide group. These modes are highly localised in the amide group, and consequently, are not very sensitive to the conformation that the chain takes. In this connection, absorption bands in the far-infrared region are of interest, particularly the amide VII band, which arises out of torsional motion around the peptide C-N bond. This kind of torsional mode of the polypeptide

skeleton involves large amplitudes of the alpha-carbon atom; vibrational coupling between adjacent units in such a motion is large, and the frequency of such a mode would be expected to depend in a very sensitive manner on the chain conformation. Vibrational studies of infinite helical chains, $(-\text{CH}_2-)_n$, $(-\text{CH}_2-\text{O}-)_n$, and $(-\text{CH}_2-\text{O}-\text{CH}_2-)_n$ have shown²¹ that the low skeletal frequencies primarily due to the torsional modes or to the bending modes are quite sensitive to the helical conformations, whereas the high frequencies primarily associated with the stretching modes do not change as much with changes in conformation. Coming to the polypeptides, infrared studies on polyglycine²² have shown that the frequency of the amide VII band differs appreciably for the two conformations in which the polypeptide exists. It should be useful, then, to search for correlations between these low-frequency modes and the helical conformations. This work has been motivated in part by the desire to try to gain information on the relationship of these modes and their dispersion to the chain conformation. Besides, dispersion curves are of use for making band assignments, and for analysing vibrational spectra of low-molecular-weight oligomers of the same structure. Useful thermodynamic quantities such as entropy and specific heat can be obtained from frequency distribution functions which are calculated from dispersion curves. Calculation of these thermodynamic quantities, while it has not been attempted as part of the present work, is the next obvious step in understanding thermodynamic properties of polypeptide systems.

REFERENCES

1. R.E. Dickerson, in "The Proteins", H. Neurath, Ed., Academic Press, New York, 1964, Vol. II, p. 603.
2. J.T. Yang, Adv. Protein Chem. 16, 323 (1961).
3. E.M. Shooter, Prog. in Biophys. and Biophys. Chem. 10, 195 (1960).
4. P. Urnes and P. Doty, Adv. Protein Chem. 16, 401 (1961).
5. E.R. Blout, in "Aspects of Protein Structure", G.N. Ramachandran, Ed., Academic Press, New York-London, 1963, p. 241.
6. J.A. Schellman and C. Schellman, in "The Proteins", H. Neurath, Ed., Academic Press, New York, 1964, Vol. II, p. 1.
7. W.F. Harrington, R. Josephs, and D.M. Segal, Annual Review of Biochemistry, 35, 599 (1966).
8. J.T. Yang, in "Conformation of Biopolymers", G.N. Ramachandran, Ed., Academic Press, New York-London, 1967, p. 157.
9. S.N. Timasheff, H. Susi, R. Townend, L. Stevens, M.J. Gorbunoff, and T.F. Kumosinski, in "Conformation of Biopolymers", G.N. Ramachandran, Ed., Academic Press, New York-London, 1967, p. 173.
10. F.A. Bovey, G.V.D. Tiers, and G. Filipovich, J. Polymer Sci. 38, 73 (1959).
11. F.A. Bovey, in "Polymer Conformation and Configuration", Academic Press, New York-London, 1969, p. 98.
12. A. Hvidt and S.O. Nielsen, Adv. Protein Chem. 21, 287 (1966).
13. W. Traub, U. Shmueli, M. Suwalsky and A. Yonath, in "Conformation of Biopolymers", G.N. Ramachandran, Ed., Academic Press, New York-London, 1967, p. 449.
14. E.J. Ambrose and A. Elliott, Proc. Roy. Soc. (London) A 205, 47 (1951).
15. P. Doty, A.M. Holtzer, J.H. Bradbury, and E.R. Blout, J. Am. Chem. Soc. 76, 4493 (1954).
16. G.R. Bird and E.R. Blout, J. Am. Chem. Soc. 81, 2499 (1959).

17. T. Miyazawa, J. Chem. Phys. 32, 1647 (1960); T. Miyazawa and E.R. Blout, J. Am. Chem. Soc. 83, 712 (1961).
18. M. Beer, G.B.B.M. Sutherland, K.N. Tanner, and D.L. Wood, Proc. Roy. Soc. (London), A 249, 147 (1958).
19. T. Miyazawa, in "Aspects of Protein Structure", G.N. Ramachandran, Ed., Academic Press, New York, 1963, p. 257.
20. T. Miyazawa, in "Poly- α -amino acids", G.D. Fasman, Ed., Dekker, New York, 1967, p. 69; Y. Masuda, K. Fukushima, T. Fujii, and T. Miyazawa, Biopolymers, 8, 91 (1969).
21. T. Miyazawa, Spectrochim. Acta 16, 1231, 1233 (1960); J. Chem. Phys. 35, 693 (1961).
22. T. Miyazawa, Bull. Chem. Soc. Japan, 34, 691 (1961).

CHAPTER II

GENERAL THEORY2.1 MOLECULAR VIBRATIONS OF FINITE MOLECULES

In this section the general concepts of the molecular dynamics of finite molecules are recalled briefly. A molecule with N atoms has $3N-6$ vibrational degrees of freedom (or $3N-5$ if the molecule is linear). In the Wilson's GF-matrix method¹, one makes use of 'internal coordinates' to describe the motion. These internal coordinates are the changes in bond lengths, bond angles and out-of-plane and dihedral angles. The use of these internal coordinates makes the problem more physically understandable. Force constants in terms of these coordinates have a more easily visualised physical meaning than others. In addition these force constants appear in certain cases at least to carry over from one similar molecule to another. The transformation to internal coordinates from Cartesian coordinates is defined, in matrix-vector notation, by

$$R = BX \quad (2.1)$$

Then, the G-matrix or inverse kinetic energy matrix is defined by the relation

$$G_{kl} = \sum_{i=1}^{3n} B_{ki} B_{li} / m_i \quad (k, l = 1, 2, \dots, 3n-6) \quad (2.2)$$

where m_i is the mass of the i^{th} atom.

The kinetic energy is then given by

$$2T = \dot{R}' G^{-1} \dot{R} \quad (2.3)$$

where R' denotes the transpose of R .

The potential energy is given by the expression

$$2V = R' F R \quad (2.4)$$

in which the elements F_{kl} are the force constants.

The molecular vibration problem is then represented by the matrix equation

$$GFL = L\lambda \quad (2.5)$$

where the vibrational frequencies are given by $\lambda = 4\pi^2 \nu^2 c^2$ and the normal coordinates Q are related to the internal coordinates R by

$$R = LQ \quad (2.6)$$

The vibrational problem thus leads to the secular equation

$$\{GF - E\lambda\} = 0 \quad (2.7)$$

which must be solved to obtain the vibrational frequencies ν .

The solution of the matrix equation (2.5) also yields the eigenvectors L of the dynamical matrix. The normal coordinates Q are related to the internal displacement coordinates by the linear transformation (2.6). The extent of vibrational coupling between the various internal displacement coordinates in a given normal mode Q_k is

quantitatively described by the elements of the eigenvector L_k belonging to the eigenvalue λ_k .

Another measure of the nature of a normal vibration is the fractional potential energy associated with each internal coordinate. The fractional potential energy of the k^{th} normal mode associated with the i^{th} internal coordinate is given by²

$$(PE)_i^k = L_{ik}^2 F_{ii} / \lambda_k \quad (2.8)$$

The potential energy distribution (P.E.D.) is useful in making assignments of various frequencies.

2.2 MOLECULAR VIBRATIONS OF POLYMER CHAINS

The basic concepts discussed in the previous section can be applied to polymer chains. However, when one considers a polymer molecule of infinite length, the dimensions of the matrices involved become infinite. In order to reduce the problem to one of workable dimensions, a few additional concepts must be introduced. The first point to be noted is that polymer chains are built up of chemical units or monomers arranged in a regularly repeating fashion. In other words, polymer chains possess screw symmetry. The importance of this essential helical symmetry of polymer molecules was first pointed out by P.W. Higgs³, who considered in a fairly general manner the vibrations of a helical molecule and used group-theoretical ideas to classify the normal modes and derive

the selection rules for Raman and infrared spectra.

According to Higgs' treatment, one considers an infinite helical molecule, built up by linking together identical units in such a way that each unit is transformed geometrically into the next by the operation $H(1, \psi)$, which is a translation through a distance 1 along the axis plus a rotation through an angle ψ about the same axis. Thus any group in the chain may be transformed into one $\pm n$ away by operating with H^n . The set of all operations H^n ($n = \text{any integer, positive or negative}$) which transform one unit into another constitutes an infinite group which is simply isomorphic with the infinite cyclic group C_∞ . Its irreducible representations are, therefore, all one-dimensional, and may be labelled $\Gamma(\theta)$ with a parameter θ which runs through all values in the range $-\pi < \theta \leq +\pi$; the corresponding characters are given by

$$\chi(\theta, H^n) = \exp(in\theta) \quad (2.9)$$

Every normal mode of vibration of the molecule must belong to one of these representations, that is, if in a normal mode a certain unit vibrates in some manner with an amplitude A , then the n^{th} unit farther on must vibrate in the same manner with an amplitude $A \exp(-in\theta)$. Each frequency ν_i of an isolated unit gives rise to a band of frequencies $\nu_i(\theta)$ in the helically linked molecule, where θ is the phase difference between the motions of adjacent units. It can be shown that to each frequency $\nu_i(\theta)$, there corresponds a

frequency $\nu_i(-\theta)$, which is equal to $\nu_i(\theta)$. Thus with the exception of $\nu_i(0)$ and $\nu_i(\pi)$ the frequencies are degenerate in pairs belonging to $\Gamma(\theta)$ and $\Gamma(-\theta)$ ($0 < \theta < \pi$); the corresponding complex normal modes may, therefore, be combined to form two real ones in which the amplitudes vary as $A \cos n\theta$ and $A \sin n\theta$.

Coming to the solution of the vibrational secular equation, let R_i^n denote the i^{th} internal displacement coordinate belonging to the n^{th} chemical unit. Then the potential interaction and kinetic coupling between the i^{th} internal coordinate of the n^{th} unit and the k^{th} internal coordinate of the n'^{th} unit are given by the matrix elements $F_{ik}^{nn'}$ and $G_{ik}^{nn'}$. Now the periodicity of the chain requires that these matrix elements depend on n and n' only through their difference, that is,

$$F_{ik}^{nn'} = F_{ik}^s \quad (2.10)$$

$$G_{ik}^{nn'} = G_{ik}^s \quad (2.11)$$

where $s = \{n - n'\}$. In view of this, a portion of the infinite G matrix can be written in terms of R 's as

	$\dots \bar{R}^{n-3}$	\bar{R}^{n-2}	\bar{R}^{n-1}	\bar{R}^n	\bar{R}^{n+1}	\bar{R}^{n+2}	$\bar{R}^{n+3} \dots$
<hr/>							
\vdots							
\bar{R}^{n-3}	G_A	G'_B	G'_C	G'_D			
\bar{R}^{n-2}	G_B	G_A	G'_B	G'_C	G'_D		
\bar{R}^{n-1}	G_C	G_B	G_A	G'_B	G'_C	G'_D	
\bar{R}^n	G_D	G_C	G_B	G_A	G'_B	G'_C	G'_D
\bar{R}^{n+1}		G_D	G_C	G_B	G_A	G'_B	G'_C
\bar{R}^{n+2}			G_D	G_C	G_B	G_A	G'_B
\bar{R}^{n+3}				G_D	G_C	G_B	G_A
\vdots							

where \bar{R}^n is the column vector of the internal coordinates of the n^{th} chemical unit. G'_A, G'_B, \dots denote the transposes of G_A, G_B, \dots . The F matrix would also have an analogous structure.

Higgs showed that the G and F matrices of an infinite order may be factored into the set of matrices $G(\delta)$ and $F(\delta)$ of a finite order, corresponding to the phase difference δ between the vibrations of adjacent units in the chain. The order of $G(\delta)$ or $F(\delta)$ is equal to N , the number of internal coordinates in a chemical repeat unit. A Fourier transform on the system of internal displacement coordinates is defined, to give a set of internal symmetry

coordinates,

$$S(\delta) = \sum_{n=-\infty}^{\infty} R^n \exp(in\delta) \quad (2.12)$$

The elements of the $G(\delta)$ and $F(\delta)$ matrices are then

$$G_{ik}(\delta) = \sum_{s=-\infty}^{\infty} G_{ik}^s \exp(is\delta) \quad (2.13)$$

$$F_{ik}(\delta) = \sum_{s=-\infty}^{\infty} F_{ik}^s \exp(is\delta) \quad (2.14)$$

The secular equation of an infinite order can then be reduced to the set of N^{th} order equations

$$\left| G(\delta) F(\delta) - \lambda(\delta) E \right| = 0 \quad (2.15)$$

where the vibrational frequencies are given by $\lambda(\delta) = 4\pi^2 c^2 \nu^2(\delta)$ (where ν is expressed in cm^{-1}) and $-\pi < \delta \leq +\pi$.

Symmetry properties and selection rules

Only very few of the infinite number of vibrational frequencies of a polymer calculated by equation (2.15) are optically active. Selection rules for such molecules were first worked out by Higgs, in terms of the phase difference δ and the angle ψ . It is well known that the only frequencies which appear as allowed fundamentals in infrared absorption are those belonging to representations $\Gamma(\theta)$ which are contained in the representation $\Gamma(\bar{M})$ which has as its basis the components of the total molecular electric dipole moment \bar{M} . It turns out that infrared absorption arises

either from the A vibrations with phase difference $\delta = 0$ (the transition moment being parallel to the helix axis) or from the $E(\Psi)$ vibrations with $\delta = \Psi$ (the transition moment being perpendicular to the axis).

As for the Raman selection rules, one is concerned with the total molecular electric polarizability α and it can be shown that Raman absorption arises from the vibrations with phase difference $\delta = 0, \Psi$ or 2Ψ .

Calculations on actual polymers

There have been numerous calculations on optically active frequencies for polymers. Liang, Krimm and coworkers⁴⁻⁸ first applied the result of the general theory of crystal spectra - that the only fundamental frequencies which are potentially active in optical absorption are the "factor group frequencies", or those in which corresponding atoms in the various unit cells move in phase - specifically to the case of several polymer chains, and made group-theoretical analyses to interpret the infrared spectra of polymers such as polyethylene, polytetrafluoroethylene, and polychlorotrifluoroethylene. The method of Higgs has been adapted to the calculation of the vibrational spectra of several polymer molecules by Miyazawa and coworkers⁹, and by Tadokoro¹⁰. They reformulated the problem in suitable ways for the calculation of the spectroscopically active fundamentals of polyoxymethylene, polypropylene, etc. A method suitable for the calculation only of the spectroscopically active

fundamentals has been also proposed by Schachtschneider and Snyder¹¹.

The normal vibration treatment for a polymer chain can be carried out in terms of the internal displacement coordinates. The method used in the vibrational analysis of polyalanine in the present study is the same as that described by Piseri and Zerbi¹², and is immediately adaptable for machine computation. In terms of internal coordinates R_i^n , the potential energy of the entire molecule in the harmonic approximation can be written as

$$2V = \sum_{\substack{n,n', \\ i,k}} F_{ik}^{nn'} R_i^n R_k^{n'} \quad (2.16)$$

Making use of the periodicity of the chain (equation (2.10)) it follows that

$$2V = \sum_{n;i,k} F_{ik}^0 R_i^n R_k^n + \sum_{\substack{n,s, \\ i,k}} (F_{ik}^s R_i^n R_k^{n+s} + F_{ki}^s R_i^n R_k^{n-s}) \quad (2.17)$$

The kinetic energy of the infinite chain can be written in an analogous way in terms of the momenta P_i^n conjugated to the coordinates R_i^n and the kinetic energy matrix G .

$$2T = \sum_{n;i,k} G_{ik}^0 P_i^n P_k^n + \sum_{\substack{n,s, \\ i,k}} (G_{ik}^s P_i^n P_k^{n+s} + G_{ki}^s P_i^n P_k^{n-s}) \quad (2.18)$$

Hamilton's equations of motion can be written using equations (2.17) and (2.18), thus leading to a system of an

infinite number of second order differential equations in the R_i^{n+s} whose solution can be assumed to be the plane wave

$$R_i^{n+s} = A_i \exp \left[-i \left(\lambda^{\frac{1}{2}} t + s\delta \right) \right] \quad (2.19)$$

Here δ is the phase shift between two equivalent internal displacement coordinates in adjacent units. Substitution of equation (2.19) into the system of differential equations yields a system of $3p$ simultaneous homogeneous linear equations (p is the number of atoms in a chemical repeat unit) in the unknowns A_i , whose nontrivial solutions are given when

$$\begin{vmatrix} G(\delta) & F(\delta) - \lambda(\delta)E \end{vmatrix} = 0 \quad (2.20)$$

where the frequencies are given by $\lambda(\delta) = 4\pi^2 c^2 \nu^2(\delta)$, and

$$G(\delta) = G^0 + \sum_s (G^s \exp(is\delta) + G^{s'} \exp(-is\delta)) \quad (2.21)$$

$$F(\delta) = F^0 + \sum_s (F^s \exp(is\delta) + F^{s'} \exp(-is\delta)) \quad (2.22)$$

Equations (2.21) and (2.22) coincide with those first given by Higgs (equations (2.13) and (2.14)) through a Fourier transform on the system of internal displacement coordinates. A calculation of $\nu(\delta)$ as a function of δ gives the dispersion curves. The function is periodic with period 2π , i.e., $\nu(\delta + 2\pi) = \nu(\delta)$. Further, $\nu(\delta) = \nu(-\delta)$, so that one can limit a study of the function to the range $0 \leq \delta \leq \pi$ which corresponds to half of the first Brillouin zone. The

infrared active frequencies correspond to $\delta = 0$ and $\delta = \psi$, while Raman active modes correspond to values of $\delta = 0, \psi, 2\psi$.

For any given phase difference δ (other than 0 or π), the $G(\delta)$ and $F(\delta)$ matrices are complex. In order to avoid the difficulties involved in handling complex numbers, methods have been devised to transform the complex matrices into equivalent real matrices by constructing suitable linear combinations of coordinates⁹. One method of transforming a complex matrix to its real matrix equivalent is through a similarity transformation. It can be shown that any complex matrix $H = M + iN$ can be replaced by the real one¹³:

$$\begin{vmatrix} M & -N \\ N & M \end{vmatrix}$$

In the present case, we can write $G(\delta) = G^R(\delta) + iG^I(\delta)$ and $F(\delta) = F^R(\delta) + iF^I(\delta)$, where $G^R(\delta)$, $F^R(\delta)$, $G^I(\delta)$, $F^I(\delta)$ are the real and imaginary parts of $G(\delta)$ and $F(\delta)$. The product $H(\delta) = G(\delta) F(\delta)$ becomes

$$\begin{aligned} H(\delta) &= \begin{vmatrix} G^R(\delta) & -G^I(\delta) \\ G^I(\delta) & G^R(\delta) \end{vmatrix} \times \begin{vmatrix} F^R(\delta) & -F^I(\delta) \\ F^I(\delta) & F^R(\delta) \end{vmatrix} \\ &= \begin{vmatrix} H^R(\delta) & -H^I(\delta) \\ H^I(\delta) & H^R(\delta) \end{vmatrix}, \end{aligned} \quad (2.23)$$

where

$$\begin{aligned} H^R(\delta) &= G^R(\delta) F^R(\delta) - G^I(\delta) F^I(\delta) \\ H^I(\delta) &= G^R(\delta) F^I(\delta) + G^I(\delta) F^R(\delta) \end{aligned} \quad (2.24)$$

The matrix $H(\delta)$ now has dimensions $2N \times 2N$. The eigenvalues, however, occur in pairs of equal values. The difficulty of dealing with complex numbers is thus avoided.

The polarization vectors, which give the components of the Cartesian displacements of the atoms in the various normal modes, are an important result of normal coordinate calculations. For the mode $\nu(\delta)$ the polarization vectors are defined by

$$q(\delta) = B^{-1}(\delta) L(\delta) \quad (2.25)$$

where the $L(\delta)$ vectors are defined as in equation (2.6).

The use of the polarization vectors is considered in the next section in connection with neutron scattering experiments.

The use of group-theoretical ideas

The importance of group-theoretical ideas in the understanding and interpretation of polymer spectra may be mentioned at this point. This arises from the fact that the symmetry of a helical polymer molecule may be described by a one-dimensional space-group. As mentioned earlier, only the normal modes in which all the unit cells vibrate in phase may be active in the infrared and Raman spectra¹⁴. It is thus sufficient spectroscopically to study the factor group

of the one-dimensional space-group, which has the translational subgroup as unit element. Considering an infinite helical molecule in which the one-dimensional crystallographic repeat unit contains n chemical units and m turns (each chemical unit contains p atoms), the basic symmetry operation is a rotation of $2m\pi/n$ about the axis of the helix followed by a translation along the axis of $1/n$ of the unit cell length. The factor group in question may be denoted by $C(2m\pi/n)$, which is isomorphic with the point group C_n . An analysis of the factor group of a polymer is useful in predicting the numbers of normal modes, their symmetry properties and infrared or Raman activity. Coupled with dichroic studies on polymer spectra, an analysis of the symmetry group of the polymer can help in the analysis and interpretation of the spectra, even in the absence of complete normal vibration calculations. Liang and coworkers⁴⁻⁷ have used these group-theoretical ideas to obtain information on the interpretation of the spectra of a large number of high polymers such as polyethylene, polytetrafluoroethylene, polystyrene, polyvinyl chloride, etc. The work has been reviewed by Krimm¹⁵. The factor group analyses of the normal modes of polyalanine in the α and β forms are presented in later chapters of this thesis.

2.3 THE USE OF NEUTRON SCATTERING

Considerable information on the low frequency motions

in polymers can be obtained from the study of inelastic neutron spectra. The usefulness of this technique arises from the fact that the energy of thermal neutrons is of the same order as that of low-frequency torsional and lattice vibrations, and their wavelength is comparable to atomic spacings. This permits small energy and momentum transfers, characteristic of lattice or chain vibrations in polymers, to be readily observed. Direct information on the characteristic frequencies of these motions can be obtained. Besides, neutron scattering involves a short-range neutron-nucleus interaction rather than an electromagnetic interaction. Therefore, the intensities of the observed molecular vibrations do not depend on the magnitude of molecular dipoles, upon polarizabilities, or upon optical selection rules. In the case of infrared or Raman spectra, the vibrational frequencies that appear are those corresponding to motions involving the fluctuations of the dipole moment or polarizability. Because of the symmetry dependent selection rules, infrared and Raman scattering techniques can provide only a part of the information regarding the dynamics of molecular systems. In order to obtain information about the entire frequency distribution, it becomes necessary to consider the overtones and combination bands, where multiphonon or anharmonic effects render the selection rules largely inoperative. Alternatively, impurity-induced spectra can also provide similar information. For inelastic neutron scattering, there exist no analogous selection rules.

This freedom enables information to be obtained about the entire frequency distribution; thus in recent years much work has been directed towards a study of low-frequency vibration spectra of polymers from neutron scattering measurements.

The basic experimental set-up

A neutron scattering experiment consists in first obtaining a monochromatic beam of neutrons, which is collimated before impinging on the sample under investigation. The scattered beam is observed at a given angle. Energy analysis of the scattered neutrons is performed by timing the flight of the neutrons to the detector. This is accomplished by "chopping" the scattered beam with a set of rotating slits. The chopper thus provides a reference time at which the neutrons can be said to initiate their flight to the detectors. Figure 1 shows a schematic representation of a neutron scattering experiment.

Theory

The formal theory of inelastic neutron scattering from phonons in crystals is well developed¹⁶. The scattering of neutrons can be classified as coherent or incoherent depending on whether interference effects are present in the scattered waves or not. The scattering of a neutron wave from a system of identical nuclei, having zero spin, no isotopes, and with a periodic arrangement would be, except for magnetic interactions with the atomic electrons, entirely coherent. For a system of identical nuclei with non-zero spin, the neutron-nucleus

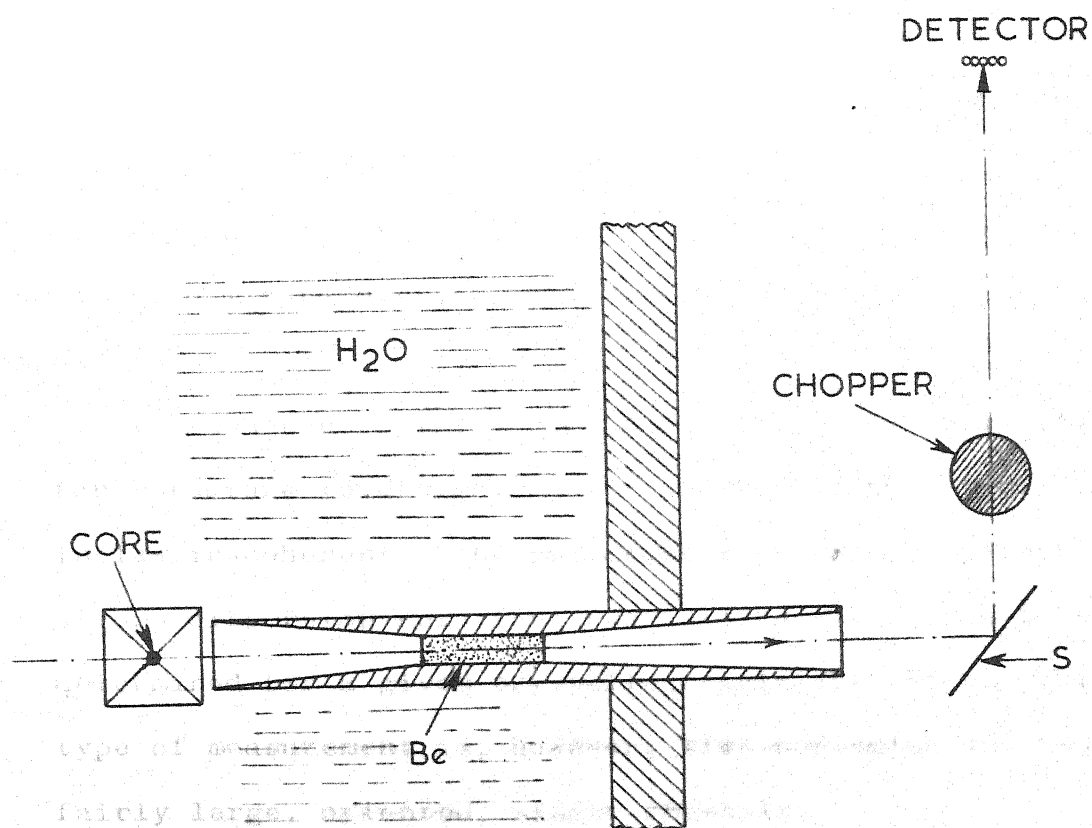


FIG. 1 SCHEMATIC OF A COLD NEUTRON FACILITY

interaction depends on the relative orientations of the neutron and nuclear spins; this can in part destroy coherence and give rise to an incoherent component. Incoherence also arises due to the existence of different spins for different isotopes. Each type of scattering (coherent and incoherent) can have an elastic and an inelastic part. Thus, the neutrons scattered from a solid may be divided into the following general components:

1. Elastic-coherent: This component is utilised primarily for structure investigations by neutron diffraction.
2. Inelastic-coherent: The measurement of this component allows dispersion relations for lattice vibrations to be determined for a given crystallographic direction. This type of measurement is, however, time-consuming and requires fairly large, oriented, single crystals.
3. Inelastic- and elastic-incoherent: Measurements of these components have comprised the majority of neutron investigations on polymers. These systems contain an appreciable amount of hydrogen nuclei. Since hydrogen scattering is essentially incoherent and the cross-section is at least an order of magnitude greater than that for other elements, the scattering from these materials is largely incoherent, and has been used to provide considerable information on molecular motions in such systems.

The fact that the interaction between the neutrons and the phonons is of short range and weak allows the use of the

Fermi pseudopotential

$$U(\bar{r}, \bar{R}_1, \dots, \bar{R}_N) = \frac{2\pi\hbar^2}{m} \sum_{l=1}^N a_l \delta(\bar{r} - \bar{R}_l) \quad (2.26)$$

where m is the neutron mass, \bar{r} and \bar{R} are neutron and nuclear position vectors and the scatterer is a system of N nuclei each labelled by the subscript l . The Fermi pseudopotential contains as a parameter the bound-nucleus scattering length a . This is a measure of the strength of the interaction. For a scattering system of identical nuclei having zero spin, a is simply a constant. If the scatterer is an isotopic mixture or if the nuclei have nonzero spin, fluctuations can occur in the scattering length. In such cases, the interactions must be treated as isotope- or spin-dependent. For nuclei with nonzero spin, the scattering length has to be modified to take into account the spin dependence of the interaction. The effect arises because the interactions in which neutron and nuclear spins are parallel are different from those in which the spins are antiparallel. The total interaction, in terms of the neutron and nuclear spin operators is then taken to be

$$U(\bar{r}, \bar{R}_1, \dots, \bar{R}_N) = \frac{2\pi\hbar^2}{m} \sum_l [a_1 + b_1(\bar{s} \cdot \bar{I}_l)] \delta(\bar{r} - \bar{R}_l) \quad (2.27)$$

where b_1 is the spin dependent scattering length and \bar{s} and \bar{I}_l are the neutron and nuclear spin operators.

The use of the Fermi approximation permits the separation of the scattering probability into a factor depending on the

initial and final neutron energy, and a "scattering law", which depends only on the molecular dynamics of the scattering system. The expression on which the theory is based is given by

$$\frac{d^2\sigma}{d\Omega dE_f} = \left(\frac{E_f}{E_o} \right)^{\frac{1}{2}} N \left[a_{coh}^2 S_c(\bar{K}, \omega) + a_{inc}^2 S_i(\bar{K}, \omega) \right] \quad (2.28)$$

Here $\frac{d^2\sigma}{d\Omega dE_f}$ is the differential scattering cross-section per unit solid angle and per unit final neutron energy, for a neutron of momentum \bar{k}_i to scatter with momentum transfer

$$\bar{K} = \bar{k}_i - \bar{k}_f \quad (2.29)$$

and energy transfer

$$\hbar\omega = E_i - E_f = \hbar^2 (k_i^2 - k_f^2)/2m \quad (2.30)$$

S_c and S_i are the scattering laws for coherent and incoherent scattering, respectively. The above expression (equation (2.28)) is for scattering from a system of N atoms which are identical except for a completely disordered distribution of nuclear spins and isotopic species. The generalisation to molecules with different atoms is straightforward. In the case of hydrogenous polymers, only the incoherent term need be considered because of the relatively large incoherent scattering cross-section of hydrogen. The "bound atom" scattering cross-section of hydrogen is about 80 barns, while for most other elements it is at least an order of magnitude smaller. Thus, in the spectra of materials

containing hydrogen, the most intense lines correspond to vibrations involving hydrogenous units, and normally only the incoherent contribution from hydrogen is considered in analysing neutron spectra of hydrogenous compounds.

For a general lattice, the differential scattering cross-section for incoherent scattering can be written as a series of terms giving the probability of absorption or emission of zero, one, or several phonons:

$$\frac{d^2\sigma_{\text{inc}}}{d\Omega dE_f} = \sum_1 \left(\frac{d^2\sigma_{\text{inc}}^{(1)}}{d\Omega dE_f} \right) \quad (2.31)$$

where 1 is the number of phonons involved in the interaction. The largest contribution to scattering is from the single-phonon ($1 = 1$) term with successive terms diminishing in magnitude. At low temperature, the main contribution to the total incoherent scattering comes only from this "one-phonon" interaction and in practical calculations, higher-order terms are neglected. This one-phonon approximation contains the assumptions that the vibrations of atoms about their equilibrium positions in the lattice are harmonic and that phonon energies $\hbar\omega$ are greater than $k_B T$.

In the one-phonon approximation, the incoherent scattering cross-section for a polycrystalline sample can be written as

where θ is the scattering angle, $a_{1\text{inc}}$ is the incoherent scattering length of the 1^{th} nucleus in the unit cell, $\exp(-2W_1)$ is the Debye-Waller factor for the 1^{th} nucleus and the sum over l includes all the n atoms in a unit cell. Here, $g_1''(\omega)$ is an effective frequency distribution, given by

$$g_1''(\omega) = \frac{m}{M_1} \frac{v}{(2\pi)^3} \frac{1}{3} \sum_j \int d^3q |\bar{c}_j^1(\bar{q})|^2 \delta[\omega - \omega_j(\bar{q})] \quad (2.33)$$

where M_1 is the mass of the 1^{th} nucleus, m is the neutron mass, v is the unit cell volume, \bar{q} is the phonon wave-vector. The index j takes on $3n$ values corresponding to the $3n$ branches of the dispersion relation. $\bar{c}_j^1(\bar{q})$ are the polarization vectors mentioned previously. Writing them in terms of the phase difference δ between adjacent chemical units, they are related to the vectors L by

$$C_j^1(\delta) = \sum_R B_{1R}^{-1}(\delta) L_j^R(\delta) \quad (2.34)$$

where $B_{1R}^{-1}(\delta)$ is the transformation from the internal coordinates R to the Cartesian coordinates.

In the case of a monoatomic polycrystalline sample, the sum over l reduces to

$$\sum_l a_{l\text{inc}}^2 \exp(-2W_l) g_l''(\omega) = a_{\text{inc}}^2 \exp(-2W) \frac{m}{M'} g''(\omega) \quad (2.35)$$

where a_{inc} is the incoherent scattering length, M' is the mass of the atom and $g''(\omega)$ is the effective frequency distribution, defined as in equation (2.33) above. The true

phonon frequency distribution may be formally defined as

$$g(\omega) = \frac{v}{(2\pi)^3} \frac{1}{3} \sum_j \int d^3q \delta [\omega - \omega_j(\bar{q})] \quad (2.36)$$

Although $g(\omega)$ and $g''(\omega)$ are not directly related, comparison of equations (2.33) and (2.36) shows that the true phonon frequency distribution function has to be weighted by the polarization vectors before it can be compared with the frequency distributions obtained from measurements of neutron scattering cross-sections.

Although the frequency distributions obtained from equation (2.32) involve the use of several approximations, they do provide useful information and are found to be in qualitative, if not quantitative, agreement with calculated distributions. While relative intensities of the contributions of the individual modes to $g(\omega)$ and the shape of the individual peaks may be inexact, the frequencies of modes can be obtained and identified.

The phase-frequency relations (dispersion curves) obtained from normal mode calculations can be of great aid in the interpretation of neutron spectra, for from these one can predict the number of maxima that should appear in the observed spectra, the frequency at which they should appear, and the types of motions involved. Conversely, relative intensities of peaks in neutron spectra can be of help in the assignment of calculated frequencies to vibrational modes in a chain. In the work on poly-L-alanine described

in Chapter IV, the inelastic neutron spectrum has been used in conjunction with the dispersion curves. The density of states function $g(\nu)$ has been calculated graphically from the one-dimensional definition

$$g(\nu) = \sum_j c_j^2(\epsilon) \left(\frac{\partial \nu_j}{\partial \epsilon} \right)^{-1} \nu_j(\epsilon) = \nu \quad (2.37)$$

where the sum is over the branches j . This has been compared with the frequency distribution obtained from inelastic neutron scattering.

REFERENCES

1. E.B. Wilson, Jr., J. Chem. Phys. 7, 1047(1939); 9, 76 (1941); E.B. Wilson, Jr., J.C. Decius, and P.C. Cross, "Molecular Vibrations", McGraw-Hill, New York, 1955.
2. Y. Morino and K. Kuchitsu, J. Chem. Phys. 20, 1809(1953); I. Nakagawa, J. Chem. Soc. Japan 74, 243 (1953).
3. P.W. Higgs, Proc. Roy. Soc. (London) A 220, 472(1953).
4. C.Y. Liang, S. Krimm, and G.B.B.M. Sutherland, J. Chem. Phys. 25, 543(1956).
5. S. Krimm, C.Y. Liang, and G.B.B.M. Sutherland, J. Chem. Phys. 25, 549(1956).
6. C.Y. Liang and S. Krimm, J. Chem. Phys. 25, 563(1956); J. Polymer Sci. 27, 241(1958); J. Mol. Spectry. 3, 554(1959).
7. S. Krimm and C.Y. Liang, J. Polymer Sci. 22, 95(1956).
8. C.Y. Liang and F.G. Pearson, J. Polymer Sci. 35, 303(1959).
9. T. Miyazawa, J. Chem. Phys. 35, 693 (1961); T. Miyazawa, K. Fukushima, and Y. Ideguchi, J. Chem. Phys. 37, 2764 (1962); T. Miyazawa, Y. Ideguchi, and K. Fukushima, J. Chem. Phys. 38, 2709 (1963).
10. H. Tadokoro, J. Chem. Phys. 33, 1558 (1960); 35, 1050(1961).
11. J.H. Schachtschneider and R.G. Snyder, Spectrochim. Acta, 20, 853(1964).
12. L. Piseri and G. Zerbi, J. Chem. Phys. 48, 3561(1968).
13. E. Bodewig, "Matrix Calculus", North-Holland, Amsterdam, 1959
14. S. Bhagavantam and T. Venkatarayudu, "Theory of Groups and its Application to Physical Problems", Andhra University, Waltair, India, 1951; M.C. Tobin, J. Chem. Phys. 23, 891 (1955).
15. S. Krimm, Fortschr. Hochpolymer-Forsch., 2, 51 (1960).
16. For example, L.S. Kothari and K.S. Singwi, Solid State Physics 8, 109 (1959); H. Boutin and S. Yip, "Molecular Spectroscopy with Neutrons", M.I.T. Press, Cambridge, 1968, and references therein.

CHAPTER III

LOW-FREQUENCY VIBRATION SPECTRA OF L-ALANINE

Next to glycine, alanine, $\text{CH}_3-\underset{\text{NH}_3}{\text{CH}}-\text{CO}_2$, is the simplest of the α -amino acids. It is also the simplest amino acid which exists in an optically active form. A study of the vibration spectra of the simple amino acids is useful first in getting information about the molecular configuration and nature of hydrogen bonding in these systems and second, in understanding and characterisation of the conformation of the polyamino acids. In the context of the present work, L-alanine is of interest since it is the monomer from which the polyalanine chain is built. This chapter presents a study of the vibration spectra of L-alanine in the low-frequency region, based principally on the infrared spectra below 600 cm^{-1} and the results obtained from inelastic neutron scattering.

Experimental

The infrared absorption spectrum of L-alanine in the form of a KBr disk has been recorded in the region from 1800 to 250 cm^{-1} using a Perkin-Elmer double beam grating spectrometer. The spectrum is shown in Figure 2. The inelastic neutron spectrum of L-alanine is shown in Figure 3. This was obtained at the AMMRC using a slow chopper. The infrared spectrum of β -alanine, $\text{CH}_2(\text{NH}_2)\text{CH}_2\text{CO}_2\text{H}$ was also obtained in this frequency region with a view to obtaining some useful information in connection with assignments. This is shown in Figure 4.

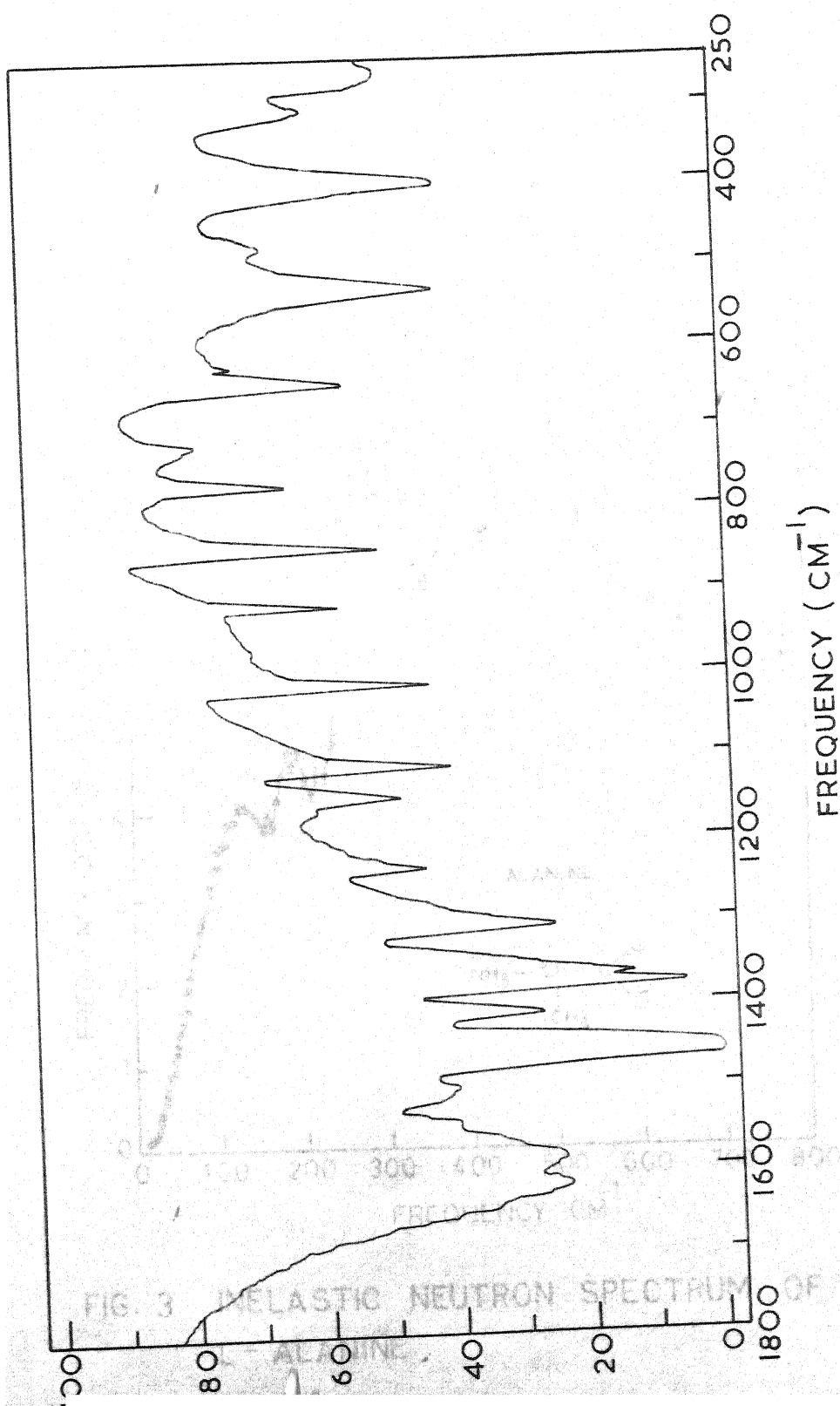


FIG. 2 INFRARED SPECTRUM OF L - ALANINE

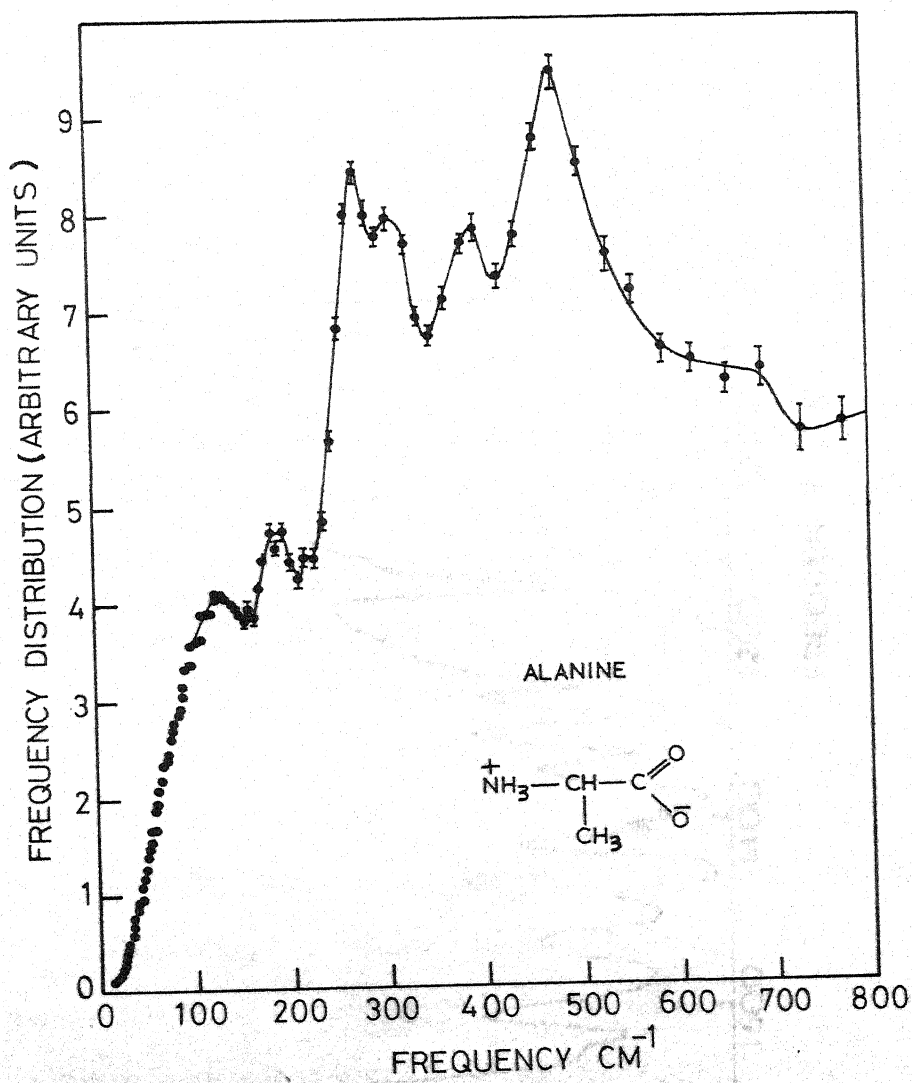


FIG. 3 INELASTIC NEUTRON SPECTRUM OF L-ALANINE.

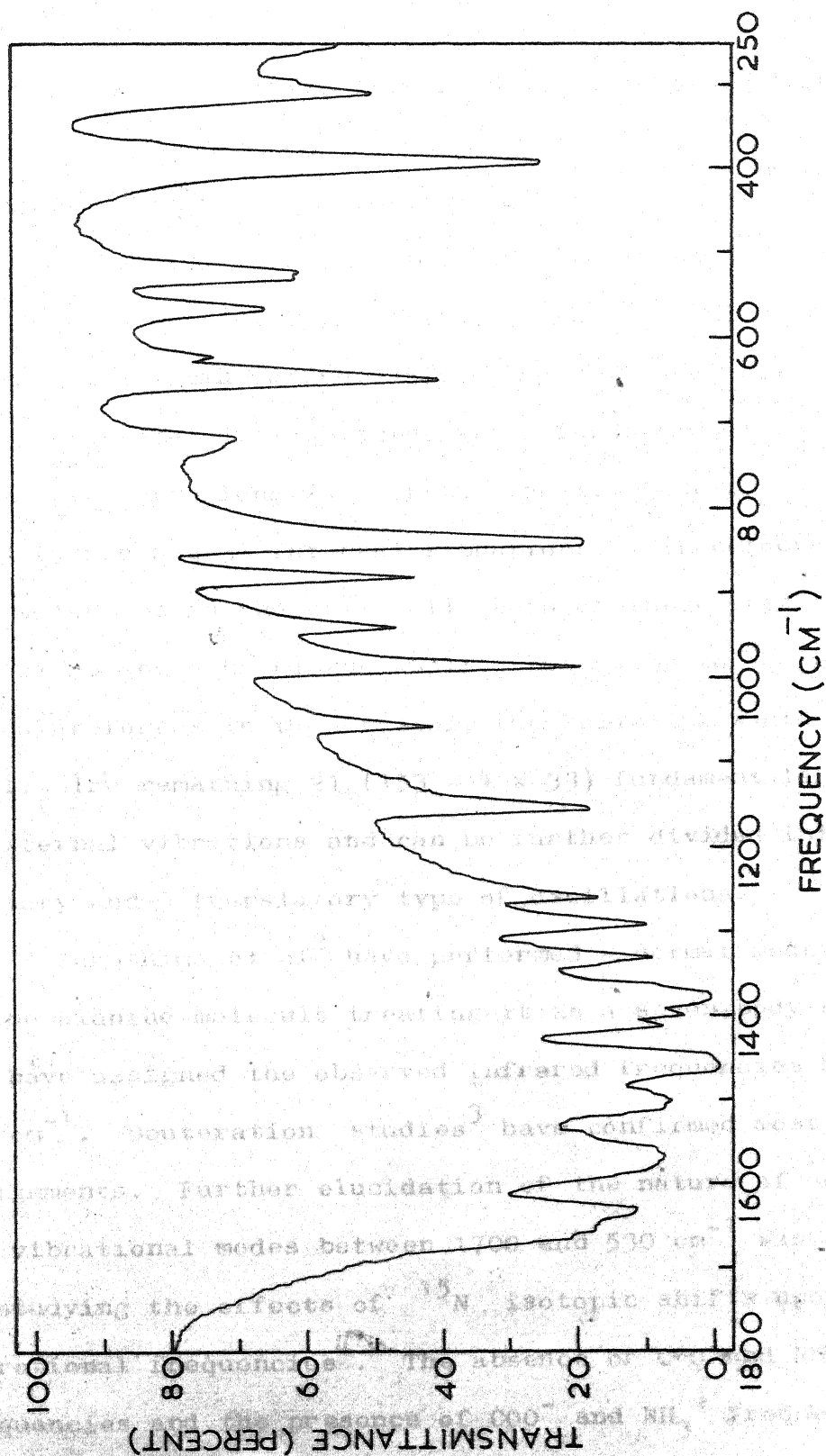


FIG. 4 INFRARED SPECTRUM OF β -ALANINE

Discussion

L-alanine crystallises in the orthorhombic form with the space group $P_{2_1 2_1 2_1}^1$. The unit cell has four molecules in it. The molecule of L-alanine and the crystal structure are shown in Figure 5. The molecule itself has no symmetry; hence all the internal vibrations of the molecule are both infrared and Raman active. Since the unit cell has 52 atoms, there is a total of 153 factor group fundamentals ($3 \times 52 - 3$), exclusive of the long-wavelength acoustic modes. Each molecule of L-alanine has 33 internal vibrations. Since there are four molecules in the unit cell, each of these internal vibrations would be further split, but owing to the weak intermolecular forces in the crystal, the splitting would be very small. The remaining 21 ($153 - 4 \times 33$) fundamentals are known as external vibrations and can be further divided into 12 rotatory and 9 translatory type of oscillations.

Fukushima et al.² have performed a normal mode calculation on the alanine molecule treating it as a seven-body problem and have assigned the observed infrared frequencies down to 600 cm^{-1} . Deuteration studies³ have confirmed most of the assignments. Further elucidation of the nature of some of the vibrational modes between 1700 and 530 cm^{-1} was obtained by studying the effects of ^{15}N isotopic shifts upon the vibrational frequencies⁴. The absence of C-O and NH_2 group frequencies and the presence of COO^- and NH_3^+ frequencies has indicated that molecules of alanine exist in the

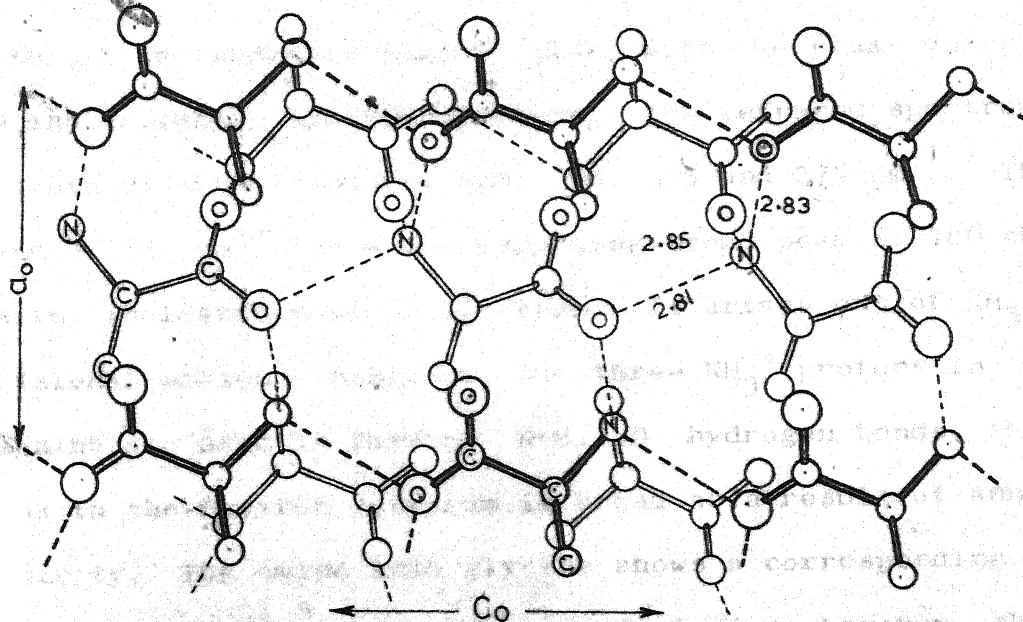
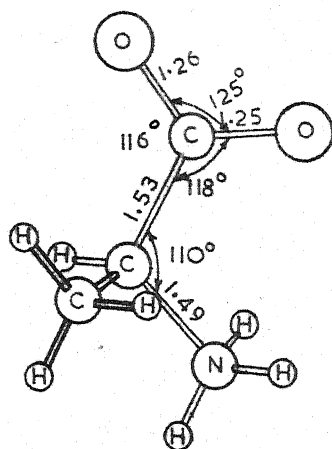


FIG. 5 MOLECULE AND CRYSTAL STRUCTURE OF L-ALANINE

'zwitterion' form, $\text{CH}_3-\underset{\text{NH}_3^+}{\underset{|}{\text{CH}}}-\text{COO}^-$. In the present study, an attempt has been made to correlate the bands observed in the infrared spectrum of L-alanine below 600 cm^{-1} with the peaks in inelastic neutron scattering and to assign the modes, taking into account the fact that the peak heights in the inelastic neutron scattering are weighted by amplitudes of the motion of hydrogen atoms. In the case of L-alanine, the modes involving large amplitudes for the hydrogen atoms are expected to be mostly the vibrations of the CH_3 and NH_3^+ groups. Since most of the CH_3 group frequencies except the torsional modes occur beyond 1000 cm^{-1} , those observed in the inelastic neutron spectrum below 600 cm^{-1} should belong to the NH_3^+ group.

The infrared bands of L-alanine in the region of interest are shown in Table 1 along with the peaks observed in the inelastic neutron spectrum. The infrared spectrum (Figure 2) shows bands at 480, 408, 315 and 275 cm^{-1} . The band at 480 cm^{-1} has a corresponding broad peak at 480 cm^{-1} in the inelastic neutron spectrum. It arises out of NH_3^+ torsional motion. Since all the three NH_3^+ protons in alanine are used in forming $\text{N-H}\cdots\text{O}$ hydrogen bonds, the peak in the neutron spectrum is broad as a result of anharmonicity. The amino acid glycine shows a corresponding similar peak at 490 cm^{-1} ⁵. In the case of glycine, however, the peak is broader. This is because of the unequal strengths of the three $\text{N-H}\cdots\text{O}$ bonds; besides, part of the broadening could be due to the occurrence of a COO^- rocking mode in the

same region (505 cm^{-1}). In alanine the corresponding mode is further removed, that is, to 540 cm^{-1} .

TABLE 1

OBSERVED INFRARED AND NEUTRON FREQUENCIES FOR L-ALANINE

Infrared (cm^{-1})	Neutron (cm^{-1})	Assignment
480	480	NH_3^+ torsion
408	395	CCN skeletal deformation
315	300	
275	270	CH_3 torsion
180 ^a	180	Skeletal torsional modes
	135	Lattice modes

^afrom Jackovitz et al.⁶.

The peaks at 408 and 315 cm^{-1} in the infrared arise out of CCN^+ skeletal deformation modes⁶. The neutron spectrum shows corresponding peaks at 395 and 300 cm^{-1} . The appreciable intensity of these peaks could be due to strong coupling of the CCN^+ bending mode with NH_3^+ rocking and possibly also with NH_3^+ torsion. The spectrum of β -alanine also shows two peaks at 395 and 312 cm^{-1} , which could be assigned to C-C-N^+ skeletal bending modes. Krishnan and Katiyar⁷ have assigned a line at 323 cm^{-1} in the Raman spectrum of β -alanine to such a bending mode.

The infrared band at 275 cm^{-1} is due to the CH_3 torsional motion. There is no corresponding band in the infrared spectrum of β -alanine, since it does not contain the CH_3 group. This mode appears as a sharp peak at 270 cm^{-1} in the neutron spectrum of L-alanine. It is also observed as a sharp peak at 267 cm^{-1} in the inelastic neutron scattering from dimethylsulphoxide⁸. The assignment to CH_3 torsion is also borne out by the fact that there is no strong peak at this frequency in the neutron spectrum for glycine, which does not have a methyl group.

The remaining broad peak at 180 cm^{-1} may be due to skeletal torsional oscillations or may arise out of lattice modes. The latter assignment is supported by the inelastic neutron spectrum of glycine, in which a strong peak at 160 cm^{-1} is assigned to a rotatory type lattice mode⁵. The infrared band at 180 cm^{-1} ⁶ corresponds to this peak. This assignment appears more reasonable than the assignment of Jackovitz et al⁶ to CH_3 torsional motion. The broad band which extends from 100 to 160 cm^{-1} is due to the lattice modes, which involve stretching and bending of hydrogen bonds. It is also broad due to anharmonicity and spreads nearly over the region of lattice modes observed in other simple amino acids which also exist in the zwitterion form⁷ and where all the three available protons are involved in hydrogen bonding. However, it should be noted that in the low-frequency region because of the width of the incident neutron beam the resolution is poor.

It is of interest to compare the features of the neutron spectrum of L-alanine with the inelastic neutron spectrum of the polymer in the α -form. This is shown in Figure 9 in the next chapter. The intense peak at 230 cm^{-1} in poly-L-alanine and the peak at 190 cm^{-1} arise out of peptide C-N torsional modes. While the peak at 270 cm^{-1} in L-alanine is certainly due to the CH_3 torsional mode, the steric hindrance between methyl groups in the packing of α -helices would reduce amplitudes of methyl torsional motion. Consequently, such an intense peak in poly-L-alanine appears more likely to arise out of C-N torsional motion. Again, the NH out-of-peptide-plane motion in α -poly-L-alanine appears as an intense peak at 610 cm^{-1} ; in L-alanine, there is no corresponding motion - the NH_3^+ torsion gives the peak at 480 cm^{-1} . The spectra in the region below 300 cm^{-1} would in general be expected to be quite different because of the basic chain structure of the polymer itself, in which the disposition and environment of peptide bonds and the N-H...O hydrogen bonds are different from the situation in L-alanine. As discussed in the next chapter, since there is a large coupling between adjacent units in the chain for vibrational modes in this region, the vibrational spectrum of the polymer would be different from that of the monomer.

REFERENCES

1. H.J. Simpson and R.E. Marsh, *Acta Cryst.*, 20, 550 (1966).
2. K. Fukushima, T. Onishi, T. Shimanouchi, and S. Mizushima, *Spectrochim. Acta*, 15, 236 (1959).
3. S. Suzuki, T. Ohshima, N. Tamiya, K. Fukushima, T. Shimanouchi, and S. Mizushima, *Spectrochim. Acta*, 15, 969 (1959); T. Ohshima and N. Tamiya, *Spectrochim. Acta*, 17, 384 (1961).
4. M. Tsuboi, T. Takenishi, and A. Nakamura, *Spectrochim. Acta*, 17, 634 (1961).
5. V.D. Gupta and R.D. Singh, *Chem. Phys. Letters*, 5, 218 (1970).
6. J.F. Jackovitz, J.A. Durkin, and J.L. Walter, *Spectrochim. Acta*, 23, 67 (1967).
7. R.S. Krishnan and R.S. Katiyar, *Bull. Chem. Soc. Japan*, 42, 2098 (1969).
8. G.J. Safford, F.C. Schaffer, P. S. Leung, G.F. Doebbler, G.W. Brady, and E.F.X. Lyden, *J. Chem. Phys.* 50, 2140 (1969).

CHAPTER IV

THE α -HELICAL FORM OF POLY-L-ALANINE

One of the most widely occurring conformations of chain molecules in biological systems is the α -helix, first proposed by Pauling and Corey¹. Pauling and his colleagues examined plausible models of polypeptide structure based on considerations of potential energy. They argued that the most stable conformation would have (1) a planar peptide unit, (2) hydrogen bonds which do not deviate much from linearity, (3) bond angles and lengths similar to those in small molecules such as amides, (4) orientation about C-C and N-C single bonds close to the potential energy minima for rotation about these bonds. The most satisfactory structure, based on the above criteria, is the α -helix, in which the peptide backbone forms a coil with a pitch (distance along the helix axis between turns) of 5.4 \AA , and a progression along the axis of 1.5 \AA per amino acid residue. Thus 5 turns of the helix contain 18 amino acid residues, that is, a turn ratio of 3.6. In other words, the α -helix has 3.6 residues per turn. Hydrogen bonds are formed between C=O and N-H groups which are three residues apart, forming rings of 13 atoms. The hydrogen bonds are nearly parallel to the helix axis. This secondary structure has been identified, both in the solid state and in solution, in a large number of polypeptides and parts of some proteins; among the former are polyalanine, poly- γ -methyl-L-glutamate and

among the latter are the fibrous proteins of the α -keratin class (hair, muscle, etc.) and globular proteins such as haemoglobin.

Structure of polyalanine chains in the α -form

Well-oriented X-ray diffraction photographs of poly-L-alanine in the α -form were obtained by C.H. Bamford et al.². However, Brown and Trotter³ noticed large discrepancies between the observed and calculated intensities, both for right- and for left-handed screw senses of the helix. The situation was clarified when Elliott and Malcolm⁴ found that all the features of the diffraction pattern could be accounted for by a hexagonal close-packed arrangement of right-handed helices in which the polar sequence CO.NH.CHR of an individual chain may point in either direction along the helix axis. In other words, the chain sense could be random. This work of Elliott and Malcolm established the right-handed α -helix for the L-enantiomorph of polyalanine. More recently, it has been shown from the consideration of steric effects⁵ that the right-handed α -helix of poly-L-alanine is energetically more stable (by a few tenths of a kilocalorie per residue) than the left-handed one. In a recent study, Parry and Suzuki^{6,7} have made a comparison of the intrachain potential energy of an infinite straight α -helix with that of the distorted form adopted in a coiled-coil conformation. The results indicate that the potential energies of the structures are almost the same, and there would be little barrier to a

transformation from one system to the other. In fact, they speculate that under certain conditions, such as in the presence of a suitable solvent, the coiled-coil rope could be regarded as a more stable structure for small assemblies of α -helices. However, no experimental evidence for such a structure for polyalanine has been reported. The α -helix of polyalanine is shown in Figure 6. Here R denotes a methyl group.

The coordinates for the atoms on the α -helix were based on the bond lengths and angles in the peptide group given by Corey and Pauling⁸. The bond lengths and bond angles are as follows:

$$\begin{aligned} r(\text{C}=\text{O}) &= 1.24 \text{ \AA}, \quad r(\text{C}-\text{N}) = 1.32 \text{ \AA}, \quad r(\text{N}-\text{H}) = 1.00 \text{ \AA}, \\ r(\text{C}_{\alpha}-\text{N}) &= 1.47 \text{ \AA}, \quad r(\text{C}_{\alpha}-\text{H}) = 1.10 \text{ \AA}, \quad r(\text{C}_{\alpha}-\text{M}) = 1.54 \text{ \AA}, \\ r(\text{C}_{\alpha}-\text{C}) &= 1.53 \text{ \AA}; \\ \phi(\text{N}-\text{C}_{\alpha}-\text{C}) &= 110^{\circ}, \quad \phi(\text{H}-\text{C}_{\alpha}-\text{C}) = 109^{\circ}, \quad \phi(\text{C}_{\alpha}-\text{C}=\text{O}) = 121^{\circ}, \\ \phi(\text{C}_{\alpha}-\text{C}-\text{N}) &= 114^{\circ}, \quad \phi(\text{O}=\text{C}-\text{N}) = 125^{\circ}, \quad \phi(\text{C}-\text{N}-\text{H}) = 123^{\circ}, \\ \phi(\text{H}-\text{N}-\text{C}_{\alpha}) &= 114^{\circ}, \quad \phi(\text{C}-\text{N}-\text{C}_{\alpha}) = 123^{\circ}, \quad \phi(\text{N}-\text{C}_{\alpha}-\text{H}) = 109^{\circ}, \\ \phi(\text{N}-\text{C}_{\alpha}-\text{M}) &= 109^{\circ}. \end{aligned}$$

Using this standard stereochemistry, Parry and Suzuki⁶ have refined the approximate coordinates originally calculated by Pauling and Corey¹. The refined values of the coordinates are shown in Table 2. From these helical coordinates, the Cartesian coordinates of the atoms were obtained and used for calculating the kinetic and potential energy matrices G and F in this work.

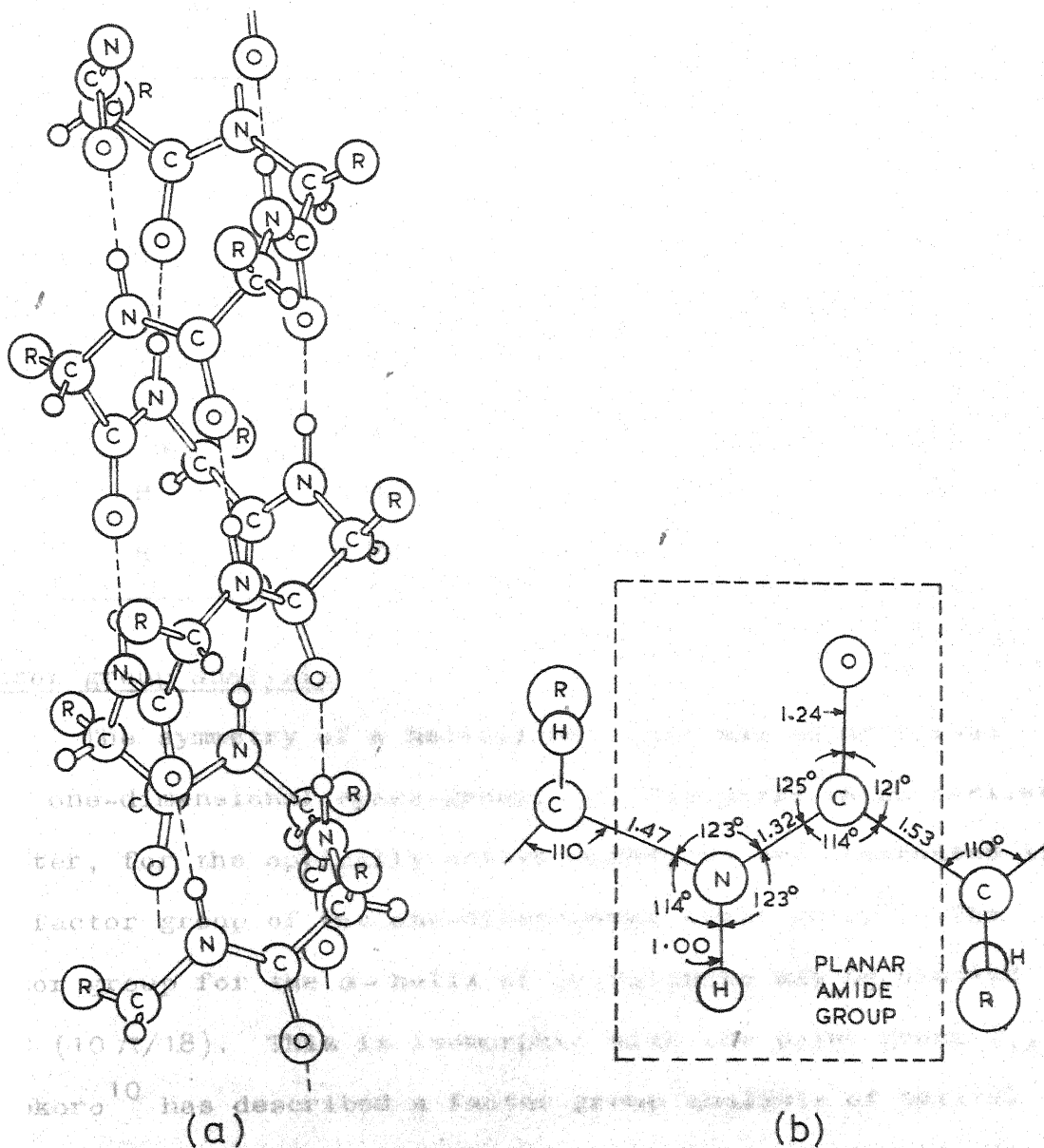


FIG. 6 (a) α -HELIX OF POLYALANINE

(b) BOND LENGTHS AND ANGLES IN THE AMIDE GROUP.

TABLE 2
COORDINATES OF ATOMS IN AN α -POLY-L-ALANINE RESIDUE⁶

	R, Å	ϕ (deg.)	z, Å
C	1.65	0.0	0.00
O	1.86	-7.7	1.20
N	1.55	45.5	-0.46
H	1.59	53.5	-1.44
C _{α}	2.28	74.1	0.41
H	3.07	61.0	0.88
R	3.22	92.8	-0.42

Factor group analysis

The symmetry of a helical molecule may be described by a one-dimensional space-group. As discussed in an earlier chapter, for the optically active modes, we are interested in the factor group of the one-dimensional space-group⁹. The factor group for the α -helix of polyalanine may be denoted as $C(10\pi/18)$. This is isomorphic with the point group C_{18} . Tadokoro¹⁰ has described a factor group analysis of helical polymer molecules in general, which can be treated under the group $C(2m\pi/n)$, where n is the number of chemical units and m , the number of turns in the one-dimensional crystallographic repeat unit of the molecule. Table 3 gives the character table, numbers of normal modes and optical activity for the $C(10\pi/18)$ factor group of the α -helix. In the table

TABLE 3

CHARACTER TABLE, NUMBERS OF NORMAL MODES AND THEIR
OPTICAL ACTIVITY FOR THE $C(10\pi/18)$ FACTOR GROUP^a

	E	C^1	C^2	C^{17}	N	I.R.	Raman
A	1	1	1	1	21(T_π , R_π)	A	A
B	1	-1	1	-1	21	F	A
E_1	2	$2\cos(5\pi/9)$	$2\cos(10\pi/9)$	42(T_σ)	A	A
E_2	2	$2\cos(10\pi/9)$	$2\cos(20\pi/9)$	42	F	A
E_3	2	$2\cos(15\pi/9)$	$2\cos(30\pi/9)$	42	F	F
\vdots	\vdots	\vdots	\vdots	\vdots	\vdots	\vdots	\vdots	\vdots
E_8	2	$2\cos(40\pi/9)$	$2\cos(80\pi/9)$	42	F	F

^a N is the number of normal modes under each irreducible representation. T_π and T_σ are pure translations parallel and perpendicular to the helix axis, respectively. R_π is a pure rotation about the axis.

A: active; F: forbidden.

The operations C^1 , C^2 , ... are as explained in the text.

the symmetry operation C^1 is a rotation of $(10\pi/18)$ about the axis of the helix followed by a translation along the axis of $1/18$ of the unit cell length. The symmetry operation C^k signifies that the screw rotation C^1 is performed k times in succession.

Treatment of the chain vibrations

The internal coordinates used in the normal vibration treatment are the following (the indices for the atoms are shown in Figure 7):

Bond stretching:

$$r(C_m=O_m), \quad r(C_m=N_m), \quad r(N_m-H_m), \quad r(N_m-C_{\alpha_m}), \quad r(C_{\alpha_m}-H_m), \\ r(C_{\alpha_m}-M_m), \quad r(C_{\alpha_m}-C_{m+1}), \quad r(O_{m-3}\dots H_m).$$

In-plane angle-bending:

$$\phi(N_{m-1}-C_{\alpha_{m-1}}-C_m), \quad \phi(H_{m-1}-C_{\alpha_{m-1}}-C_m), \quad \phi(M_{m-1}-C_{\alpha_{m-1}}-C_m), \\ \phi(C_{\alpha_{m-1}}-C_m=O_m), \quad \phi(C_{\alpha_{m-1}}-C_m-N_m), \quad \phi(O_m=C_m-N_m), \\ \phi(C_m-N_m-H_m), \quad \phi(H_m-N_m-C_{\alpha_m}), \quad \phi(C_m-N_m-C_{\alpha_m}), \quad \phi(N_m-C_{\alpha_m}-H_m), \\ \phi(N_m-C_{\alpha_m}-M_m), \quad \phi(H_m-C_{\alpha_m}-M_m), \quad \phi(C_m=O_m\dots H_{m+3}), \\ \phi(N_m-H_m\dots O_{m-3}).$$

Out-of-plane angle-bending:

$$\phi'(N_m-H_m\dots O_{m-3}), \quad \omega(C_m=O_m), \quad \omega(N_m-H_m).$$

Internal rotation:

$$t(C_m-N_m), \quad t(N_m-C_{\alpha_m}), \quad t(C_{\alpha_m}-C_{m+1}).$$

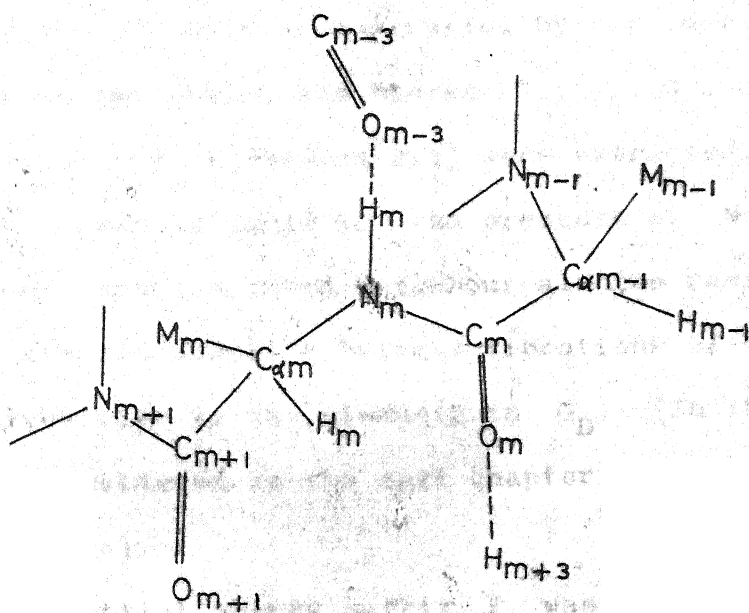
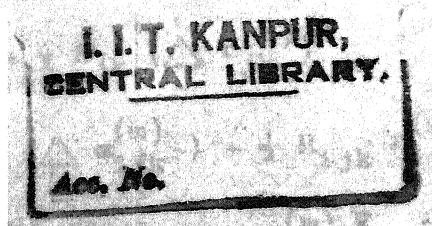


FIG. 7 PORTION OF α -HELICAL STRUCTURE
SHOWING INDICES OF THE ATOMS



here 'in-plane' and 'out-of-plane' are with reference to the plane of the peptide group. $\phi(\text{N-H}\dots\text{O})$ and $\phi'(\text{N-H}\dots\text{O})$ are the two $(\text{N-H}\dots\text{O})$ angle bending coordinates, the former in the plane of the amide group in which the N-H bond is situated, and the latter at right angles to it.

From the G matrix constructed by considering 9 residues along the chain, the blocks G_A , G_B , G_C , G_D (which have been explained in section 2.2) were extracted. The elements are shown in Table 4. The presence of N-H...O hydrogen bonds between third neighbour alanine residues introduces kinetic coupling between vibrations of these units, and this gives rise to the elements in G_D . (In the case of the β -form, considered in the next chapter, the elements of G_D are all zero).

The potential energy matrix F was derived using a Urey-Bradley force field. The Urey-Bradley potential function for the α -helical chain of poly-L-alanine can be expressed as

$$\begin{aligned}
 V = & \sum_{m,j,k} K'_{jk} r_{jk}^{(m)} (\Delta r_{jk}^{(m)}) + \frac{1}{2} K_{jk} (\Delta r_{jk}^{(m)})^2 \\
 & + \sum_{m,i,j,k} H'_{ijk} r_{ij}^{(m)} r_{jk}^{(m)} (\Delta \alpha_{ijk}^{(m)}) + \frac{1}{2} H_{ijk} r_{ij}^{(m)} r_{jk}^{(m)} (\Delta \alpha_{ijk}^{(m)})^2 \\
 & + \sum_{m,i,j,k} F'_{ik} q_{ik}^{(m)} (\Delta q_{ik}^{(m)}) + \frac{1}{2} F_{ik} (\Delta q_{ik}^{(m)})^2 \\
 & + \sum_{m,j} K_j^t (\Delta t_j^{(m)})^2 + \sum_{m,j} K_j^\omega (\Delta \omega_j^{(m)})^2. \quad (4.1)
 \end{aligned}$$

where $\Delta r_{jk}^{(m)}$, $\Delta \alpha_{ijk}^{(m)}$, $\Delta t_j^{(m)}$ and $\Delta \omega_j^{(m)}$ are the

TABLE 4

G MATRIX ELEMENTS FOR α -POLY-L-ALANINE*

I	J	G(I,J)	I	J	G(I,J)	I	J	G(I,J)	I	J	G(I,J)
<u>G_A</u>											
1	1	0.146	1	2	-0.048	1	9	-0.025	1	10	0.046
1	11	-0.023	1	12	-0.047	1	13	0.098	1	14	-0.052
1	15	-0.052	1	17	0.052	1	21	-0.009	2	2	0.155
2	3	-0.031	2	4	-0.039	2	9	0.027	2	10	-0.049
2	11	0.024	2	12	0.104	2	13	-0.050	2	14	-0.055
2	15	-0.064	2	16	0.105	2	17	-0.041	2	18	0.014
2	19	-0.039	2	21	0.050	2	22	0.064	2	25	-0.001
2	27	-0.011	2	28	0.032	3	3	1.063	3	4	-0.037
3	8	-0.992	3	13	0.049	3	14	-0.049	3	15	-0.048
3	16	-0.042	3	17	0.090	3	18	-0.014	3	19	0.040
3	24	0.003	3	25	-0.003	3	26	0.001	3	27	0.008
3	28	-0.031	4	4	0.155	4	5	-0.027	4	6	-0.028
4	7	-0.028	4	13	-0.045	4	14	0.045	4	15	0.106
4	16	-0.061	4	17	-0.045	4	18	-0.072	4	19	-0.051
4	20	0.069	4	22	-0.062	4	23	-0.002	4	25	-0.001
4	28	-0.019	5	5	1.075	5	6	-0.036	5	7	-0.024
5	16	-0.017	5	17	0.019	5	18	-0.054	5	19	0.060
5	20	-0.049	5	24	-0.049	5	25	0.053	5	26	-0.060
5	27	0.099	5	28	-0.069	6	6	0.150	6	7	-0.023
6	16	0.051	6	17	-0.051	6	18	0.071	6	19	-0.053
6	20	-0.068	6	24	0.015	6	25	-0.017	6	26	0.019
6	27	-0.076	6	28	0.088	7	7	0.167	7	16	-0.038
7	17	0.036	7	18	0.058	7	19	0.048	7	20	0.058
7	24	0.038	7	25	-0.042	7	26	0.047	7	27	-0.025
8	8	1.055	9	9	0.168	9	10	-0.001	9	11	-0.013
9	12	0.057	9	13	-0.054	9	14	-0.003	9	15	0.008

*(see footnote at the end of the table).

(contd.)

Table 4 (contd.)

I	J	G(I,J)	I	J	G(I,J)	I	J	G(I,J)	I	J	G(I,J)
9	17	-0.009	9	21	0.025	9	24	0.075	9	25	-0.036
9	26	-0.070	9	27	-0.041	10	10	0.991	10	11	-0.010
0	12	-0.107	10	13	0.102	10	14	0.006	10	15	-0.017
0	17	0.017	10	21	-0.019	10	24	0.007	10	25	-0.003
0	26	-0.007	10	27	-0.004	11	11	0.154	11	12	0.050
1	13	-0.047	11	14	-0.003	11	15	0.010	11	17	-0.009
1	21	-0.004	11	24	-0.078	11	25	0.037	11	26	0.070
1	27	0.043	12	12	0.209	12	13	-0.082	12	14	-0.128
2	15	-0.012	12	17	0.012	12	21	0.131	12	24	-0.001
3	13	0.193	13	14	-0.111	13	15	-0.129	13	16	0.004
3	17	0.125	13	18	-0.007	13	19	0.019	13	21	0.006
3	22	0.024	13	23	0.002	13	24	-0.002	13	25	0.003
3	26	-0.001	13	27	0.007	13	28	-0.016	14	14	0.239
4	15	0.141	14	16	-0.004	14	17	-0.137	14	18	0.007
4	19	-0.019	14	21	-0.137	14	22	-0.024	14	23	-0.002
4	24	0.002	14	25	-0.003	14	26	0.001	14	27	-0.006
4	28	0.016	15	15	1.204	15	16	-1.096	15	17	-0.107
5	18	-0.003	15	19	0.005	15	21	-0.027	15	22	-1.636
5	24	-0.007	15	25	0.018	15	27	0.006	15	28	-0.005
6	16	1.190	16	17	-0.093	16	18	0.037	16	19	-0.104
6	20	-0.047	16	22	1.637	16	23	0.044	16	24	-0.005
6	25	0.021	16	26	-0.004	16	27	-0.048	16	28	0.092
7	17	0.200	17	18	-0.038	17	19	0.099	17	20	0.046
7	21	0.002	17	22	-0.002	17	23	0.002	17	25	0.002
7	26	-0.001	17	27	0.052	17	28	-0.090	18	18	0.997
8	19	-0.021	18	20	-0.494	18	22	0.009	18	23	-0.046
8	24	0.119	18	25	-0.170	18	26	0.106	18	27	-0.174
8	28	0.127	19	19	0.160	19	20	-0.014	19	22	-0.024
9	23	0.015	19	24	-0.036	19	25	0.052	19	26	-0.031
9	27	0.102	19	28	-0.097	20	20	0.997	20	24	0.037
0	25	-0.040	20	26	0.045	20	27	-0.014	20	28	-0.036

(contd.)

Table 4 (contd.)

I	J	G(I,J)	I	J	G(I,J)	I	J	G(I,J)	I	J	G(I,J)
21	21	0.463	21	24	0.067	21	25	-0.020	21	26	-0.015
21	27	-0.023	22	22	2.474	22	24	0.001	22	25	-0.021
22	26	0.001	22	27	-0.008	22	28	0.020	23	23	2.474
23	24	-0.108	23	25	1.721	23	26	-0.069	23	27	0.108
23	28	-0.036	24	24	0.462	24	25	-0.415	24	26	0.073
24	27	-0.345	24	28	0.092	25	25	1.540	25	26	-0.187
25	27	0.395	25	28	-0.132	26	26	0.191	26	27	-0.136
26	28	0.082	27	27	0.410	27	28	-0.220	28	28	0.326

G_B											
1	7	-0.043	1	27	-0.043	1	28	0.014	2	7	-0.034
2	27	0.044	2	28	-0.015	3	28	0.002	4	28	-0.001
9	2	0.028	9	3	-0.029	9	4	-0.051	9	5	0.048
9	6	0.048	9	7	-0.053	9	13	-0.013	9	14	0.014
9	15	-0.002	9	16	0.077	9	17	-0.071	9	18	-0.003
9	19	-0.013	9	20	-0.120	9	22	0.017	9	23	0.035
9	24	-0.090	9	25	0.128	9	26	-0.079	9	27	0.072
9	28	0.069	10	4	0.058	10	5	-0.052	10	6	0.061
10	7	-0.073	10	16	0.060	10	17	-0.060	10	18	-0.403
10	19	-0.112	10	20	-0.402	10	24	0.003	10	25	-0.003
10	26	0.004	10	27	-0.097	10	28	0.082	11	4	0.048
11	5	0.052	11	6	-0.052	11	7	-0.052	11	16	-0.011
11	17	0.013	11	18	-0.112	11	19	-0.009	11	20	-0.004
11	24	-0.046	11	25	0.051	11	26	-0.057	11	27	0.121
11	28	-0.141	12	4	-0.027	12	5	0.052	12	6	-0.026
12	7	-0.057	12	16	-0.018	12	17	0.018	12	18	-0.021
12	19	0.050	12	20	-0.026	12	24	-0.026	12	25	0.028
12	26	-0.031	12	27	0.111	12	28	-0.062	13	4	0.028
13	5	-0.052	13	6	0.025	13	7	-0.057	13	16	0.017
13	17	-0.018	13	18	0.021	13	19	-0.050	13	20	0.027

(contd.)

Table 4 (contd.)

I	J	G(I,J)	I	J	G(I,J)	I	J	G(I,J)	I	J	G(I,J)
13	24	0.026	13	25	-0.028	13	26	0.031	13	27	-0.107
13	28	0.059	14	7	0.115	14	27	-0.005	14	28	0.001
15	7	0.057	15	27	0.016	15	28	-0.011	16	28	-0.002
17	7	-0.057	17	27	-0.015	17	28	0.007	18	28	0.038
19	28	-0.011	21	7	-0.053	21	27	0.009	21	28	0.026
22	28	0.001	23	28	-0.059	24	7	0.001	24	27	-0.051
24	28	0.259	25	7	-0.001	25	27	0.024	25	28	-0.228
26	4	0.047	26	5	0.005	26	6	-0.050	26	16	-0.024
26	17	0.024	26	18	-0.062	26	19	0.004	26	20	0.061
26	24	-0.006	26	25	0.007	26	26	-0.008	26	27	0.052
26	28	-0.049	27	7	-0.001	27	27	0.028	27	28	-0.183
28	28	0.029									

 G_C

9	28	-0.030
---	----	--------

 G_D

8	1	-0.061	8	12	-0.012	8	14	0.012	8	21	-0.013
22	1	-0.001	22	12	0.014	22	14	-0.014	22	21	0.116
22	24	-0.024	23	1	0.008	23	12	-0.023	23	14	0.023
23	21	-0.880	23	24	-0.013						

Only nonzero elements are listed. The numbering of the internal coordinates is in accordance with the order in which they are listed in the text.

For G_A , which is symmetric, only elements on the main diagonal and above it are listed.

internal coordinates corresponding to bond stretch, angle bend, torsion and out-of-peptide plane wag, respectively. The subscripts on the first three internal coordinates label the atoms involved and the superscript m labels the chemical repeat unit. The torsional coordinate $\Delta t_j^{(m)}$ is the skeletal torsion about the j^{th} bond. The interactions across the hydrogen bonds have also been taken into account in the above expression. The force field for the β -structure of polyalanine was first obtained (This is described in Chapter V.). It is reasonable to expect that some of the potential constants, particularly those pertaining to vibrations localised in the amide group, should be transferable to the case of the α -form without appreciable alteration. The force field was, therefore, based initially on that for the β -form and then modified to get agreement with infrared observed frequencies. The force constants of acetylglycine N-methylamide, $\text{CH}_3\text{CONHCH}_2\text{CONHCH}_3$ ¹¹, were also of use in modifying the force field. The force constants associated with the hydrogen bond were modified from those obtained for crystalline N-methylacetamide¹². The force constants are shown in Table 5. The F-matrix elements are given in Table 6. The secular equation (2.20) was solved for values of the phase difference δ ranging from 0 to π in steps of 0.1π . The dispersion curves were thus obtained.

TABLE 5

FORCE CONSTANTS FOR α -POLY-L-ALANINE

	mdyne/ \AA	
$K(C=O)$	7.91	
$K(C-N)$	4.96	
$K(N-H)$	5.12	
$K(N-C_{\alpha})$	3.41	
$K(C_{\alpha}-H)$	3.96	
$K(C_{\alpha}-M)$	2.22	
$K(C_{\alpha}-C)$	2.30	

	H, mdyne/ \AA	F, mdyne/ \AA		mdyne. \AA
$(N-C_{\alpha}-C)$	0.32	0.50	$\omega(C=O)$	0.53
$(H-C_{\alpha}-C)$	0.24	0.48	$\omega(N-H)$	0.19
$(M-C_{\alpha}-C)$	0.25	0.40	$t(C-N)$	0.45
$(C_{\alpha}-C=O)$	0.25	0.60	$t(N-C_{\alpha})$	0.02
$(C_{\alpha}-C-N)$	0.21	0.60	$t(C_{\alpha}-C)$	0.05
$(O=C-N)$	0.47	0.90		
$(C-N-H)$	0.27	0.50	<u>Hydrogen bond</u>	
$(H-N-C_{\alpha})$	0.28	0.47		mdyne/ \AA
$(C-N-C_{\alpha})$	0.50	0.35	$K(O...H)$	0.16
$(N-C_{\alpha}-H)$	0.17	0.80	$H(N-H...O)$	0.04
$(N-C_{\alpha}-M)$	0.27	0.50	$H(C=O...H)$	0.01
$(H-C_{\alpha}-M)$	0.23	0.40		

TABLE 6

F MATRIX ELEMENTS FOR α -POLY-L-ALANINE*

<u>I</u>	<u>J</u>	<u>F(I,J)</u>	<u>I</u>	<u>J</u>	<u>F(I,J)</u>	<u>I</u>	<u>J</u>	<u>F(I,J)</u>	<u>I</u>	<u>J</u>	<u>F(I,J)</u>
<u>F_A</u>											
1	1	8.640	1	2	1.192	1	12	0.236	1	14	0.584
1	21	0.312	2	2	5.231	2	3	0.397	2	13	0.281
2	14	0.732	2	15	0.217	2	17	0.143	3	3	6.010
3	8	0.027	3	15	0.191	3	16	0.223	4	4	3.820
4	5	0.312	4	6	0.246	4	7	0.245	4	17	0.253
4	19	0.182	5	5	4.731	5	6	0.312	5	7	0.312
5	18	0.201	5	19	0.201	6	6	2.793	6	7	0.182
6	19	0.175	6	20	0.278	7	7	4.431	8	8	0.160
9	9	0.960	9	10	-0.090	9	11	-0.090	10	10	0.421
10	11	-0.090	11	11	0.910	12	12	0.550	13	13	0.652
14	14	0.971	15	15	0.456	16	16	0.597	17	17	1.042
18	18	0.392	18	19	-0.090	18	20	-0.090	19	19	0.522
19	20	-0.090	20	20	0.441	21	21	0.010	22	22	0.040
23	23	0.040	24	24	0.530	25	25	0.190	26	26	0.450
27	27	0.020	28	28	0.050						
<u>F_B</u>											
1	7	0.467	2	7	0.629	9	4	0.012	9	7	0.013
9	18	-0.090	9	19	-0.090	10	5	0.137	10	7	0.186
10	18	-0.090	10	20	-0.090	11	6	0.316	11	7	0.314
11	19	-0.090	11	20	-0.090	12	7	0.336	13	7	0.526
<u>F_D</u>											
8	1	0.197									

* Only nonzero elements are listed. The numbering of the internal coordinates is in accordance with the order in which they are listed in the text (p. 50).

Experimental

For the α -helix, the A species vibrations, which correspond to the phase difference $\delta = 0$, and the E species vibrations, which correspond to $\delta = 5\pi/9$ are infrared active. The calculated values of the optically active frequencies were fitted by comparison with observed infrared frequencies. The infrared absorption spectrum of α -polyalanine in the form of a KBr disk obtained here using a Perkin Elmer 521 spectrometer in the region $4000 - 250 \text{ cm}^{-1}$ is shown in Figure 8. Itoh and coworkers¹³ have obtained infrared spectra of α -polyalanine below 1700 cm^{-1} and have made some polarization studies on oriented films. Elliott¹⁴, in his studies on the infrared spectra of synthetic polypeptides with small side-chains, has also made polarization studies in the region above 800 cm^{-1} . Information obtained from these studies has been made use of in modifying the force field and making assignments of bands. Koenig and Sutton¹⁵ have obtained the laser-excited Raman spectrum of α -poly-L-alanine. The results of their studies as well as those of Fanconi et al.¹⁶ have been of help in confirming some of the assignments. The inelastic neutron spectrum of α -poly-L-alanine obtained at the AMRC was also of help in connection with assignments of frequencies. The frequency distribution obtained from measurements of inelastic neutron scattering is shown in Figure 9.

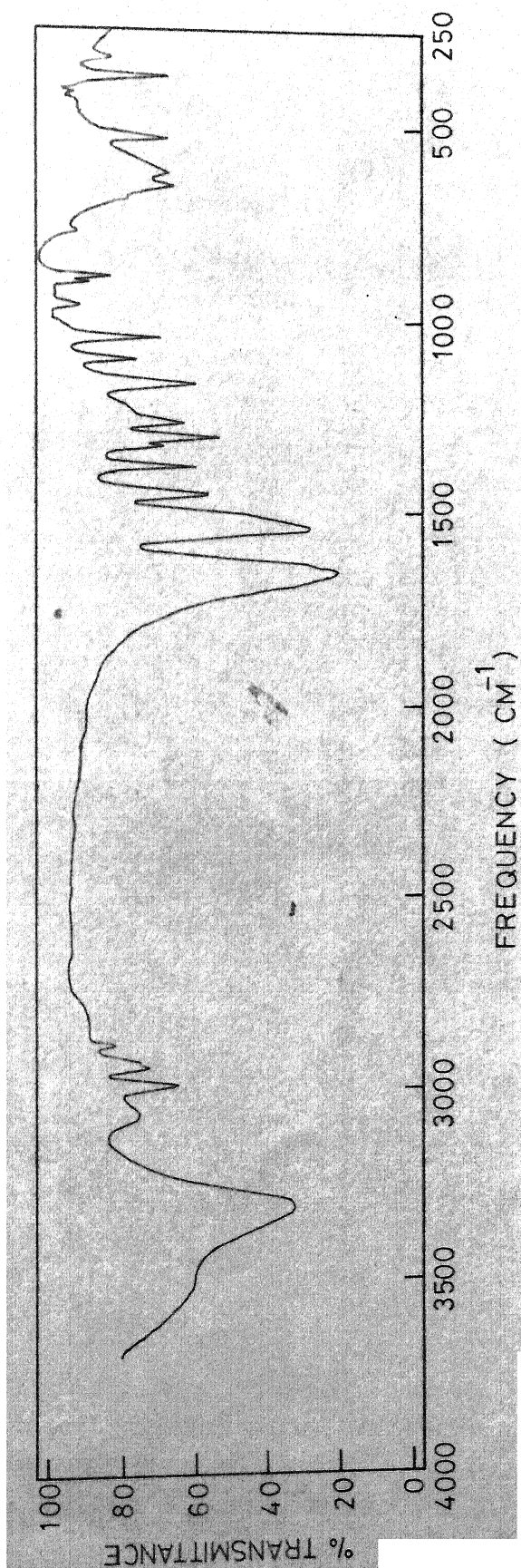


FIG. 8 INFRARED SPECTRUM OF α -POLY-L-ALANINE

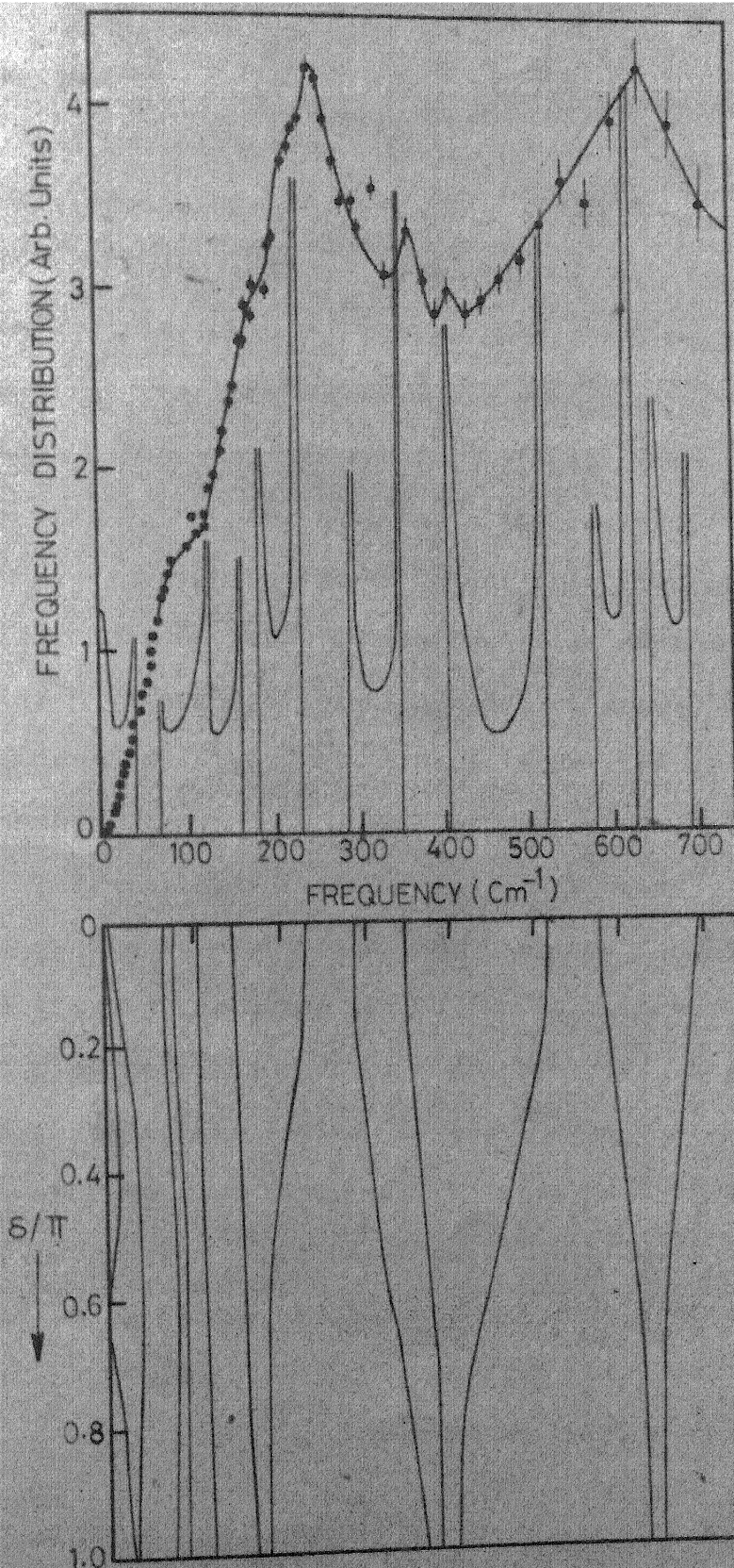


FIG. 9 DISPERSION CURVES AND FREQUENCY DISTRIBUTION FOR α -HELIX OF POLY-L-ALANINE.

Discussion

The calculated frequencies of the A vibrations with phase difference $\delta = 0$ and the E vibrations with phase difference $\delta = 5\pi/9$ are shown, along with the observed frequencies, in Table 7. The potential energy distributions (P.E.D.) for the various modes are also shown. The assignments are made on the basis of the P.E.D.'s for the different modes. The fact that the peak heights in the inelastic neutron spectrum are weighted by amplitudes of motion of hydrogen atoms (that is, intense peaks in the inelastic neutron spectrum are associated with modes in which hydrogen atoms participate to a considerable extent) is of help in confirming some of the assignments.

The optically active frequencies below 900 cm^{-1} are of importance in connection with conformation studies on polypeptides. The amide V band, which arises out of the N-H out-of-peptide-plane bending mode, has been shown to be useful for conformational studies¹⁷. The E mode calculated at 618 cm^{-1} corresponds to this band. The intense peak at 610 cm^{-1} in the inelastic neutron spectrum is due to this mode. It also appears as an intense peak in the neutron spectra of polyglycine^{18,19}. The amide VII band, which arises from torsional motion around the peptide C-N bond, is expected to be of use in the characterisation of conformations. The perpendicular band at 185 cm^{-1} in the infrared spectrum¹³ can be assigned to this torsional mode, the E species frequency of which is calculated at 184 cm^{-1} .

TABLE 7

CALCULATED AND OBSERVED FREQUENCIES FOR α -POLY-L-ALANINEa) A vibrations (phase difference = 0°)^a

calculated	Observed (ir)	Assignment ^b (P.E.D. (%))
3295	3293	r(N-H) (92)
2890	2883 ^c	r(C _{α} -H) (99)
1655	1659 ^c	r(C=O) (60), r(C-N) (21) (Amide I)
1521	1515	ϕ (C-N-H)(41), ϕ (C _{α} -N-H)(33), r(C-N)(21) (Amide II)
1318	1330 ^c	ϕ (H-C _{α} -M)(37), ϕ (H-C _{α} -C)(18)
1268	1270 ^c	ϕ (C _{α} -N-H)(20), ϕ (C-N-H)(18), r(C _{α} -C)(21), r(C-N)(12) (Amide III)
953	..	r(C _{α} -M)(32), r(C _{α} -C)(17), ϕ (M-C _{α} -C)(18)
868	907 ^c	r(C _{α} -C)(38), r(C-N)(27), r(N-C _{α})(10)
748	..	ω (N-H)(37), ϕ (O=C-N)(10), ϕ (N-C-C _{α})(15), ω (C=O)(12)
691	685 ^c	ω (C=O)(55), ϕ (C-C _{α} -M)(11), ω (N-H)(10) (Amide VI)
581	595	ω (N-H)(61), ϕ' (N-H...O)(10), ω (C=O)(10) (Amide V)
521	525 ^c	ϕ (O=C-N)(32), ϕ (C _{α} -C-N)(18), ϕ (O=C-C _{α})(16) (Amide IV)
352	350 ^d	ϕ (M-C _{α} -C)(30), ϕ (M-C _{α} -N)(15), ω (C=O)(10)
286	284 ^c	ϕ (M-C _{α} -N)(28), ϕ (M-C _{α} -C)(15), ϕ (O=C-N)(11), ϕ (O=C-C _{α})(12)
230	238 ^d	t(C-N)(39), ϕ (H-C _{α} -C)(12), ϕ (M-C _{α} -C)(8), ϕ (H-C _{α} -N)(6), ϕ (C-N-C _{α})(6), t(C _{α} -C)(7) (Amide VII)
145	120	r(O...H)(43), ϕ (N-H...O)(10)
104	100 ^d	ϕ' (N-H...O)(44), t(C-N)(8), ϕ (N-H...O)(9)
78	..	t(C _{α} -C)(34), t(N-C _{α})(25), t(C-N)(8)
65	60 ^d	ϕ (N-H...O)(38), r(O...H)(11), ϕ (H-N-C _{α})(9)

Foot-note at the end of the table.

(contd.)

Table 7 (contd.)

b) E vibrations (phase difference = 100°)^a

Calculated	Observed(ir)	Assignment ^b (F.E.D.(%))
3295	3293	r(N-H)(95)
2890	2883 ^c	r(C _α -H)(99)
1651	1659 ^c	r(C=O)(65), r(C-N)(18) (Amide I)
1542	1540 ^c	δ(C-N-H)(40), δ(C _α -N-H)(29), r(C-N)(23) (Amide II)
1310	1305 ^c	δ(H-C _α -M)(35), δ(H-C _α -C)(20)
1278	1274	δ(C-N-H)(20), δ(C _α -N-H)(23), r(C _α -C)(18), r(C-N)(10), (Amide III)
1087	1108	r(C _α -M)(40), δ(M-C _α -C)(26), r(C _α -C)(16), δ(H-C _α -M)(11)
886	893	r(C _α -C)(36), r(N-C _α)(21), r(C-N)(23)
770	782	ω(N-H)(32), ω(C=O)(21), δ(N-C _α -C)(11), δ(M-C _α -C)(11)
651	656 ^c	ω(C=O)(39), ω(N-H)(16), δ'(N-H...O)(8) (Amide VI)
618	610 ^{c,d}	ω(N-H)(51), ω(C=O)(18), δ'(N-H...O)(7) (Amide V)
458	440	δ(O=C-N)(28), δ(O=C-C _α)(23), δ(C _α -C-N)(16), (Amide IV)
367	375 ^c	δ(M-C _α -C)(28), δ(N-C _α -C)(18)
332	325	δ(M-C _α -N)(24), δ(M-C _α -C)(21), δ(O=C-N)(13), δ(O=C-C _α)(9)
184	190 ^d	t(C-N)(28), δ(N-C _α -C)(10), δ(M-C _α -C)(12), δ(H-C _α -M)(7), (Amide VII)
164	167	r(O...H)(36), δ(N-H...O)(12)
113	113	δ'(N-H...O)(41), δ(C-N-H)(9)
92	90	t(C _α -C)(29), t(N-C _α)(25), t(C-N)(19)
79	80 ^d	δ(N-H...O)(34), r(O...H)(7), δ(H-N-C _α)(8)
37	..	t(N-C _α)(11), t(C _α -C)(9), δ(N-H...O)(12), δ(N-C _α -C)(7), etc.

^a All frequencies are in cm⁻¹.^b r: bond stretching; δ: in-plane angle bend; ω, δ': out-of-peptide-plane angle bend. Only major contributions to the F.E.D. are listed.^c Frequencies also observed in the Raman spectrum¹⁵.^d Frequencies observed in inelastic neutron scattering.

The neutron spectrum shows a corresponding shoulder at 190 cm^{-1} . The calculated A species frequency for this mode is at 230 cm^{-1} . The peak at 230 cm^{-1} in the neutron spectrum is due to this vibrational mode. This peak does not seem likely to correspond to a CH_3 torsional motion, although in the monomer L-alanine the intense peak at 270 cm^{-1} is assigned to such a mode. This is because of the steric hindrance between the methyl groups in neighbouring chains of polyalanine which would be expected to reduce the amplitudes of methyl torsional oscillations; consequently the peak due to such a motion would not be very intense in the inelastic neutron spectrum.

The helix deformation modes involving stretches and bends of the $\text{N-H}\dots\text{O}$ hydrogen bonds appear in the region below 200 cm^{-1} . The mode with its A end at 145 cm^{-1} consists primarily of a stretching motion of the $\text{O}\dots\text{H}$ bond. Two modes appear which are associated with bending of the $\text{N-H}\dots\text{O}$ linear bond, in one case, the bending taking place mostly in the plane of the amide group in which the N-H bond is situated and in the other, mostly out of this plane. The peaks in the inelastic neutron spectrum at 60 and 80 cm^{-1} ²⁰ may be due to these modes. There is, besides, a low-frequency skeletal torsional mode arising out of a mixture of skeletal torsions. While the A end of this mode is largely made up of $\text{C}_\alpha\text{-C}$ and N-C_α torsions, the potential energy distribution at the E end shows a considerable mixing with the C-N torsion as well. There is, in addition, a certain amount of mixing of

the torsional modes with the angle bending modes of the helix. This is to be expected as a result of the non-planarity of the conformation. Such mixing is not obtained in the case of the β -form of polyalanine, discussed in the next chapter.

Very recently, calculations on the dispersion curves of the α -helix of polyalanine have been reported by Itoh and Shimanouchi²¹. There is, in general, agreement with the present calculations, except for a few differences in the region below 200 cm^{-1} . Our calculation shows in this region two helix deformation modes arising largely from bending motions of the N-H...O hydrogen bonds. These modes are not calculated by Itoh and Shimanouchi. For the lower of these two there is no infrared data available. However, the inelastic neutron spectrum of poly-L-alanine²⁰ shows two weak peaks at 60 and 80 cm^{-1} which could correspond to this mode. As regards the higher of these modes, in view of the dichroic measurements reported by Itoh and Shimanouchi, it appears that the perpendicular 113 cm^{-1} band could correspond to the E end of this mode, calculated in the present work at 113 cm^{-1} , rather than to the E end of the low-frequency torsional mode, which is at 90 cm^{-1} in both calculations; the shoulder in the spectrum for α -polyalanine at 90 cm^{-1} reported by Itoh et al.¹³ may be associated with this torsional mode. The A end of this N-H...O deformation mode is reflected in the shoulder in the inelastic neutron spectrum (Figure 9) at 100 cm^{-1} . Substitution studies should help in

clarifying the assignment in this region.

The mode which disperses from 748 to 770 cm^{-1} in our calculations is different from the calculations of Ithand Shimanouchi. However, the observed infrared band at 782 cm^{-1} and the Raman lines at 756 and 767 cm^{-1} ¹⁶ seem to bear out our calculations. This also agrees with the calculations of the optically active frequencies reported by Miyazawa²² on normal and deuterated polyalanines.

The dispersion curves are shown in Figure 9 for the frequency branches below 700 cm^{-1} , which exhibit appreciable dispersion. The two lowest-lying curves (with $\nu = 0$ at $\delta = 0$) are the acoustic branches. They are reduced to non-genuine vibrations at $\delta = 0$, namely, the translational mode along the chain axis and rotational mode about the axis. The lower acoustic branch is a non-genuine vibration at $\delta = \psi$, corresponding to the translational mode perpendicular to the axis.

An interesting feature of the dispersion curves is their tendency to come closer together in groups near the E end. This is indicative of the coupling between various modes for phase values near the helix angle ψ . Similar behaviour is seen in the dispersion curves of polytetrafluoroethylene (15/7 helix) recently published²³. For the α -helix of poly-L-alanine, this feature is prominent for the N-H and C=O wagging modes in the region around 650 cm^{-1} and for the bending modes in the neighbourhood of 400 cm^{-1} , in which angles around

the α -carbon atom are involved. All these modes involve motion of the nitrogen atoms. In the case of polytetrafluoroethylene, this effect is seen for the stretching motions of the CF_2 group around 1200 cm^{-1} and for the low-frequency bending modes involving motion of the fluorine atoms. It thus seems reasonable to suppose that in both systems the effect can be attributed to the presence of strong intramolecular interactions stabilising the helical structure. In the α -helix we have the intrachain hydrogen bonds, while in polytetrafluoroethylene, there is strong interaction between the fluorine atoms. The dispersion curves of polyglycine II^{19,24} (which exists as a 3-fold helix and does not have strong intrachain interactions of this nature), do not show this feature.

The calculation of frequency distribution functions is one of the uses of dispersion curves, and this has been outlined in Chapter II. The frequency distribution obtained for the isolated α -helix of polyalanine after weighting by the amplitudes of hydrogen atoms is also plotted in Figure 9. This may be compared with the frequency distribution obtained from inelastic neutron scattering. In view of the approximations involved in deriving the frequency distribution from inelastic neutron scattering measurements, it is hard to make quantitative conclusions; however, on the whole the regions of higher density of states agree with the predictions from the calculations on the isolated chain. For more realistic analyses

of the neutron scattering peaks, calculations must be done on a three-dimensional system.

The dispersion curves and the inelastic neutron spectrum for polyglycine I have already been reported¹⁸. In connection with the present work, the amplitude-weighted frequency distribution for the polyglycine I chain was also calculated, particularly with a view to studying the validity of single chain models for such calculations. In Figure 10, the frequency distribution calculated from the dispersion curves of polyglycine I is superposed on the frequency distribution derived from measurements of inelastic neutron scattering cross-sections. Here also the calculated peak frequencies agree well with frequencies of scattering peaks. It must, however, be mentioned that in both the cases, particularly in the region below 200 cm^{-1} , where the effect of lattice vibrations becomes significant, a more realistic comparison of the frequency distributions may be made only when lattice modes are taken into account, that is, when calculations are done on an actual crystal.

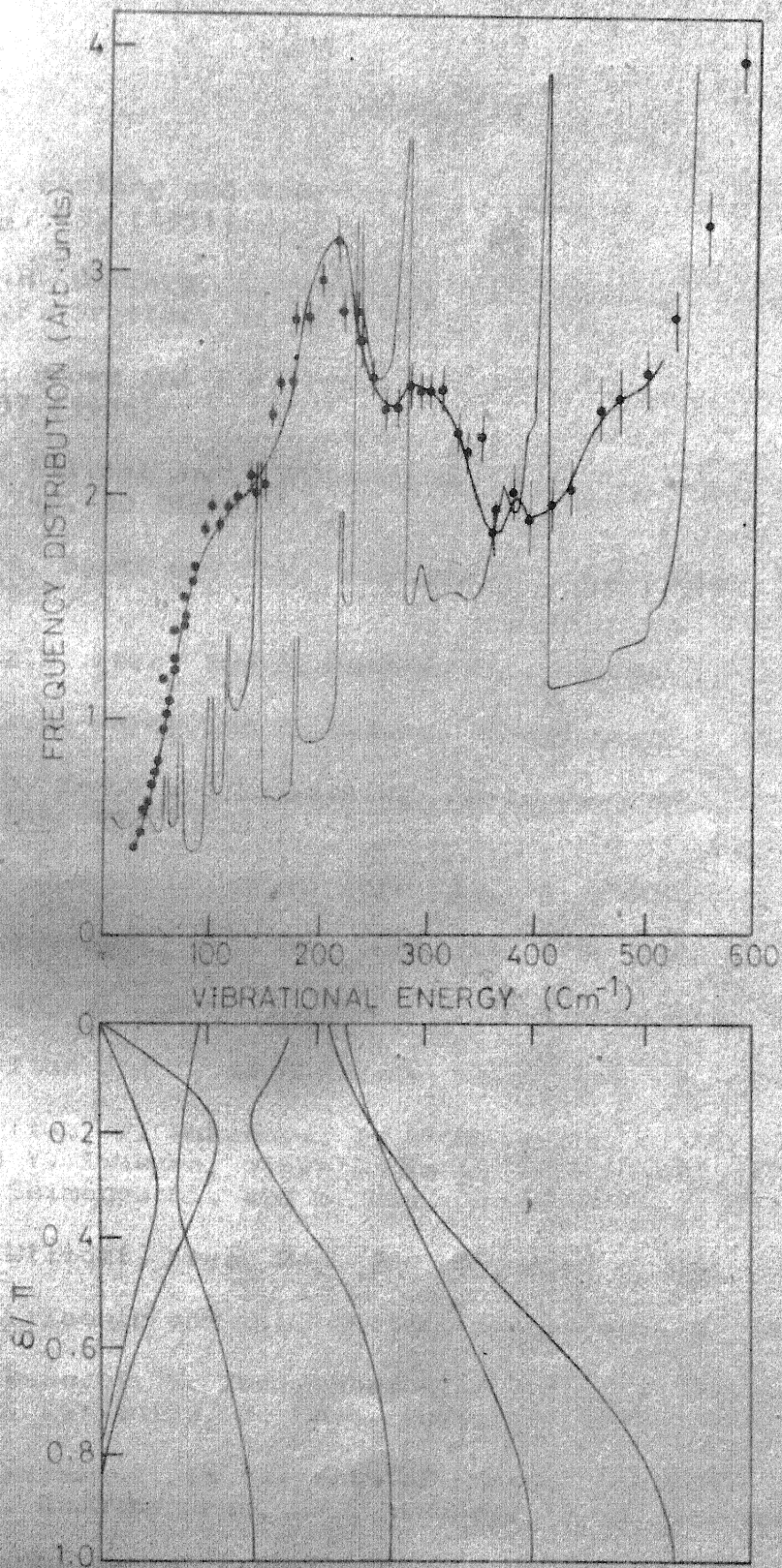


FIG. 10 DISPERSION CURVES AND FREQUENCY DISTRIBUTION FOR POLYGLYCINE I

REFERENCES

1. L. Pauling and R.B. Corey, Proc. Natl. Acad. Sci. 37, 235 (1951).
2. C.H. Bamford, L. Brown, A. Elliott, W.E. Hanby, and I.F. Trotter, Nature 173, 27 (1954).
3. L. Brown and I.F. Trotter, Trans. Faraday Soc. 52, 537 (1956).
4. A. Elliott and B.R. Malcolm, Proc. Roy. Soc. (London) A 249, 30 (1959).
5. R.A. Scott and H.A. Scheraga, J. Chem. Phys. 45, 2091 (1966).
6. D.A.D. Farry and E. Suzuki, Biopolymers 7, 189 (1969).
7. D.A.D. Farry and E. Suzuki, Biopolymers 7, 199 (1969).
8. R.B. Corey and L. Pauling, Proc. Roy. Soc. (London) B 141, 10 (1953).
9. M.C. Tobin, J. Chem. Phys. 23, 891 (1955).
10. H. Tadokoro, J. Chem. Phys. 33, 1558 (1960).
11. Y. Koyama and T. Shimanouchi, Biopolymers 6, 1037 (1968).
12. K. Itoh and T. Shimanouchi, Biopolymers 5, 921 (1967).
13. K. Itoh, T. Nakahara, T. Shimanouchi, M. Oya, K. Uno, and Y. Iwakura, Biopolymers 6, 1759 (1968); K. Itoh, T. Shimanouchi, and M. Oya, Biopolymers 7, 649 (1969).
14. A. Elliott, Proc. Roy. Soc. (London) A 226, 408 (1954).
15. J.L. Koenig and P.L. Sutton, Biopolymers 8, 167 (1969).
16. B. Fanconi, B. Tomlinson, L.A. Nafie, W. Small, and W.L. Peticolas, J. Chem. Phys. 51, 3993 (1969).
17. T. Miyazawa, in "Aspects of Protein Structure", G.N. Ramachandran, Ed., Academic Press, New York, 1963, p.257.
18. V.D. Gupta, S. Trevino, and H. Boutin, J. Chem. Phys. 48, 3008 (1968).

19. R.D. Singh and V.D. Gupta, Spectrochim. Acta (in press).
20. V.D. Gupta, H. Boutin, and S. Trevino, Nature 214, 1325 (1967).
21. K. Itoh and T. Shimanouchi, Biopolymers 9, 383 (1970).
22. T. Miyazawa, K. Fukushima, S. Sugano, and Y. Masuda, in "Conformation of Biopolymers", G.N. Ramachandran, Ed., Academic Press, New York, 1967, Vol. 2, p. 557.
23. M.J. Hannon, F.J. Boerio, and J.L. Koenig, J. Chem. Phys. 50, 2829 (1969).
24. E.W. Small, B. Fanconi, and W.L. Peticolas, J. Chem. Phys. 52, 4369 (1970).

CHAPTER V

THE β -FORM OF POLY-L-ALANINE

In addition to helical conformations, polypeptides are also stable in the form of fully-extended or nearly fully-extended chains, known as the β -form. In this, hydrogen bonding takes place between the N-H groups of one chain and the C=O groups of the chains on either side, so making a sheet held together by hydrogen bonds. Neighbouring sheets are then held together by van der Waals' forces. Fauling and Corey, in their studies of plausible models of polypeptides structure, proposed the parallel and anti-parallel chain pleated sheet structures¹⁻³. These consist of chains in a nearly fully-extended conformation, the small contraction from the fully-extended chain being produced by slight rotation about the single bonds of the α -carbon atom. These β -structures have been identified in films and fibres of synthetic polypeptides, in fibrous proteins, and in silk fibroin, the protein of silk. The structural features common to all β -structures (irrespective of the side-chains) are (a) a repeat of pattern of the polypeptide backbone along the chain axis of 7 \AA or somewhat less; (b) an interchain distance of about 4.7 \AA in the direction of the hydrogen bond; (c) C=O and N-H bonds nearly at right angles to the chain axis; (d) a two-fold screw axis (for the polypeptide backbone) along the chain axis.

The β -structure of poly-L-alanine

Bamford and coworkers⁴ obtained X-ray diffraction photographs of a highly oriented specimen of poly-L-alanine and concluded the existence of the β -form of this polypeptide. Their results were confirmed by the observations of Brown and Trotter⁵; the question of relative chain directions, however, was not settled with certainty. More recently, Arnott et al.⁶ have carried out similar studies on β -poly-L-alanine with a view to refining the structure. It has been shown to consist of pleated sheets in which the chains are arranged in an anti-parallel manner. The observed repeat distance of 6.9 \AA along the fibre-axis can be better explained on the basis of an anti-parallel chain model; besides, this leads to more linear inter-chain hydrogen bonds. The observed features of the X-ray diffraction diagrams have been explained on the basis of a statistical structure, with neighbouring sheets displaced relative to each other at random by $\pm \frac{1}{2}$ the interchain distance. The normal modes of vibration of an isolated, infinite chain in the β -structure have been calculated in this chapter.

Factor group analysis

The extended chain of β -polyalanine possesses a two-fold screw axis. The one-dimensional crystallographic repeat unit (unit cell) contains 2 chemical units and one turn. Each chemical unit contains 7 atoms, so that, with the symbols used in the previous chapter, $n = 2$, $m = 1$, $p = 7$. The chain can, therefore, be treated under the factor group $C(2m\pi/n) = C(\pi)$,

which is isomorphic with the point group C_2 . The character table for this group, the numbers of normal modes and their optical activity are shown in Table 8. The symmetry operation C^1 denotes a rotation by π about the axis of the chain followed by a translation of $\frac{1}{2}$ of the unit cell length. There are 19 nonzero fundamentals for $\delta = 0$ and for $\delta = 180^\circ$.

TABLE 8

CHARACTER TABLE, NUMBERS OF NORMAL MODES AND THEIR OPTICAL ACTIVITY FOR THE $C(\pi)$ FACTOR GROUP*

	E	C^1	N	Infrared	Raman
A	1	1	21 (T_z, R_z)	A	A
B	1	-1	21 (T_x, T_y)	A	A

*N is the number of normal modes under each irreducible representation.

T_z is a pure translation parallel to the chain axis. T_x, T_y are pure translations perpendicular to the chain axis. R_z is a pure rotation about the chain axis.

Treatment of the chain vibrations

The unit cell of a polyalanine chain in the β -form is shown in Figure 11. The coordinates of the atoms in the extended chain were calculated using bond lengths and angles based on the data of Corey and Pauling⁷. The latter have been listed in the previous chapter. The internal coordinates used in the normal vibration treatment are as follows:

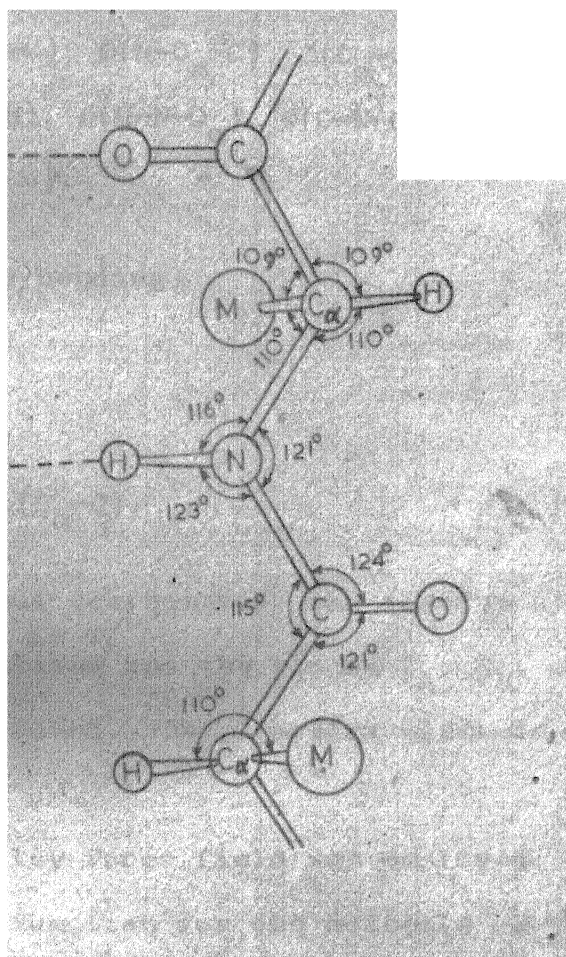


FIG. 11. UNIT CELL OF POLYALANINE CHAIN IN THE β FORM.

Bond stretching:

$$r(C=O), r(C-N), r(N-H), r(N-C_{\alpha}), r(C_{\alpha}-H), r(C_{\alpha}-M), r(C_{\alpha}-C).$$

In-plane angle bending:

$$\begin{aligned} &\phi(N-C_{\alpha}-C), \phi(H-C_{\alpha}-C), \phi(M-C_{\alpha}-C), \phi(C_{\alpha}-C=O), \phi(C_{\alpha}-C-N), \\ &\phi(O=C-N), \phi(C-N-H), \phi(H-N-C_{\alpha}), \phi(C-N-C_{\alpha}), \phi(N-C_{\alpha}-H), \\ &\phi(N-C_{\alpha}-M), \phi(H-C_{\alpha}-M). \end{aligned}$$

Out-of-plane angle bending:

$$\omega(C=O), \omega(N-H).$$

Internal rotation:

$$t(C-N), t(N-C_{\alpha}), t(C_{\alpha}-C).$$

Using these internal coordinates, the inverse kinetic energy matrix G was calculated and the blocks G_A , G_B , of dimensions 24×24 , were extracted. The G matrix elements are shown in Table 9.

A Urey-Bradley force field was employed. The Urey-Bradley potential function for the molecule of polyalanine can be expressed as in equation (4.1). To start with, the potential energy matrix was based on the force field for β -polyalanine used by Miyazawa in his calculations⁸. Some of the force constants were transferred from polyglycine I⁹. The force field was modified to get agreement with the infrared observed frequencies. The force constants are shown in Table 10. The elements of the potential energy matrix are shown in Table 11.

TABLE 9

G MATRIX ELEMENTS FOR β -POLY-L-ALANINE*

I	J	G(I,J)	I	J	G(I,J)	I	J	G(I,J)	I	J	G(I,J)
G_A											
1	1	0.146	1	2	-0.048	1	8	0.046	1	9	-0.024
1	10	-0.024	1	11	-0.046	1	12	0.098	1	13	-0.052
1	14	-0.052	1	16	0.052	2	2	0.155	2	3	-0.039
2	4	-0.039	2	8	-0.049	2	9	0.025	2	10	0.025
2	11	0.104	2	12	-0.049	2	13	-0.055	2	14	-0.060
2	15	0.101	2	16	-0.041	2	17	0.020	2	18	0.030
3	3	1.063	3	4	-0.029	3	12	0.045	3	13	-0.045
3	14	-0.045	3	15	-0.044	3	16	0.090	3	17	-0.022
4	4	0.155	4	5	-0.028	4	6	-0.028	4	7	-0.028
4	12	-0.045	4	13	0.045	4	14	0.111	4	15	-0.065
4	16	-0.045	4	17	-0.071	4	18	-0.051	4	19	0.062
5	5	1.075	5	6	-0.027	5	7	-0.027	5	15	-0.027
5	16	0.027	5	17	-0.053	5	18	0.053	5	19	-0.051
5	21	0.046	5	22	-0.055	5	23	-0.034	5	24	0.045
6	6	0.150	6	7	-0.027	6	15	-0.027	6	16	0.027
6	17	0.063	6	18	-0.053	6	19	-0.072	6	21	-0.046
6	22	0.055	6	23	0.034	6	24	-0.045	7	7	0.167
7	15	0.053	7	16	-0.053	7	17	0.063	7	18	0.053
7	19	0.059	8	8	0.167	8	9	-0.007	8	10	-0.017
8	11	-0.105	8	12	0.099	8	13	0.006	8	14	-0.017
8	16	0.017	9	9	0.991	9	10	-0.005	9	11	0.055
9	12	-0.052	9	13	-0.003	9	14	0.008	9	16	-0.008
9	20	-0.137	9	21	-0.038	9	22	-0.074	9	23	-0.042
10	10	0.156	10	11	0.053	10	12	-0.050	10	13	-0.003
10	14	0.008	10	16	-0.008	10	20	0.134	10	21	0.038
10	22	0.070	10	23	0.042	11	11	0.210	11	12	-0.080

*For footnote see at the end of the table.

(contd.)

Table 9 (contd.)

I	J	G(I,J)	I	J	G(I,J)	I	J	G(I,J)	I	J	G(I,J)
11	13	-0.130	11	14	-0.013	11	16	0.013	12	12	0.192
12	13	-0.112	12	14	-0.135	12	15	0.009	12	16	0.125
12	17	-0.010	12	18	-0.010	13	13	0.242	13	14	0.147
13	15	-0.009	13	16	-0.138	13	17	0.010	13	18	0.010
14	14	1.211	14	15	-1.093	14	16	-0.118	15	15	1.175
15	16	-0.082	15	17	0.054	15	18	0.052	15	19	0.058
16	16	0.200	16	17	-0.055	16	18	-0.052	16	19	-0.058
17	17	0.995	17	18	-0.010	17	19	-0.439	17	20	-0.030
17	21	-0.154	17	22	0.099	17	23	-0.011	17	24	-0.078
18	18	0.160	18	19	-0.004	18	20	0.030	18	21	0.150
18	22	-0.093	18	23	0.014	18	24	0.074	19	19	0.984
19	21	0.009	19	22	-0.010	19	23	-0.006	19	24	0.008
20	20	0.472	20	21	0.271	20	22	0.083	20	23	0.214
20	24	0.037	21	21	1.535	21	22	-0.180	21	23	0.230
21	24	0.167	22	22	0.189	22	24	-0.095	23	23	0.214
23	24	0.080	24	24	0.189						

 G_B

1	7	-0.042	2	7	-0.033	8	2	-0.040	8	3	0.044
8	4	-0.051	8	5	0.053	8	6	0.053	8	7	-0.053
8	12	0.020	8	13	-0.020	8	15	-0.103	8	16	0.104
8	17	-0.010	8	18	-0.019	8	19	-0.114	9	4	0.062
9	5	-0.051	9	6	0.058	9	7	-0.071	9	15	-0.036
9	16	0.036	9	17	-0.439	9	18	-0.114	9	19	-0.412
9	21	-0.046	9	22	0.054	9	23	0.065	9	24	-0.004
10	4	0.051	10	5	0.049	10	6	-0.051	10	7	-0.051
10	15	-0.024	10	16	0.024	10	17	-0.114	10	18	-0.013
10	19	-0.001	10	21	0.041	10	22	-0.049	10	23	-0.062
11	4	0.050	11	5	-0.026	11	6	-0.026	11	7	-0.057
11	15	0.012	11	16	-0.012	11	17	-0.034	11	18	-0.022

(contd.)

Table 9 (contd.)

1	J	G(I,J)	I	J	G(I,J)	I	J	G(I,J)	I	J	G(I,J)
11	19	0.056	12	4	-0.050	12	5	0.026	12	6	0.026
12	7	-0.057	12	15	-0.012	12	16	0.012	12	17	0.034
12	18	0.022	12	19	-0.056	13	7	0.115	14	7	0.057
16	7	-0.057	17	24	0.034	18	24	-0.034	20	5	0.039
20	6	-0.039	20	17	-0.041	20	18	0.037	20	19	0.007
20	21	0.032	20	22	-0.039	20	23	-0.144	20	24	-0.163
21	23	-0.047	21	24	-0.208	22	5	0.048	22	6	-0.048
22	17	-0.050	22	18	0.046	22	19	0.008	22	21	0.040
22	22	-0.048	22	23	-0.061	22	24	0.056	23	23	-0.051
23	24	-0.131	24	24	-0.042						

Only nonzero elements are listed. The numbering of the internal coordinates is in accordance with the order in which they are listed in the text (p.78).

For G_A , which is symmetric, only elements on the main diagonal and above it are listed.

TABLE 10
FORCE CONSTANTS FOR β -POLY-L-ALANINE

	mdyne/Å [°]	
K(C=O)	7.45	
K(C-N)	5.81	
K(N-H)	4.89	
K(N-C _α)	3.23	
K(C _α -H)	4.25	
K(C _α -M)	2.27	
K(C _α -C)	2.35	

	H, mdyne/Å [°]	F, mdyne/Å [°]		mdyne. Å [°]
(N-C _α -C)	0.48	0.50		
(H-C _α -C)	0.28	0.48		
(M-C _α -C)	0.43	0.40		
(C _α -C=O)	0.28	0.60		
(C _α -C-N)	0.24	0.60	ω(C=O)	0.60
(O=C-N)	0.45	0.90	ω(N-H)	0.24
(C-N-H)	0.30	0.50	t(C-N)	0.26
(H-N-C _α)	0.31	0.47	t(N-C _α)	0.06
(C-N-C _α)	0.51	0.35	t(C _α -C)	0.08
(N-C _α -H)	0.14	0.80		
(N-C _α -M)	0.22	0.50		
(H-C _α -M)	0.23	0.40		

TABLE 11

F MATRIX ELEMENTS FOR β -POLY-L-ALANINE*

I	J	F(I,J)	I	J	F(I,J)	I	J	F(I,J)	I	J	F(I,J)
<u>F_A</u>											
1	1	8.280	1	2	1.068	1	11	0.220	1	13	0.696
2	2	6.060	2	3	0.381	2	12	0.275	2	13	0.611
2	14	0.227	2	16	0.152	3	3	6.633	3	14	0.191
3	15	0.204	4	4	3.600	4	5	0.328	4	6	0.211
4	7	0.211	4	17	0.296	4	18	0.190	5	5	5.080
5	6	0.328	5	7	0.328	5	17	0.216	5	19	0.216
6	6	2.810	6	7	0.195	6	18	0.182	6	19	0.290
7	7	4.502	8	8	1.300	8	9	-0.090	8	10	-0.090
9	9	0.508	9	10	-0.090	10	10	1.200	11	11	0.613
12	12	0.711	13	13	0.882	14	14	0.542	15	15	0.628
16	16	1.103	17	17	0.301	17	18	-0.090	17	19	-0.090
18	18	0.453	18	19	-0.090	19	19	0.446	20	20	0.600
21	21	0.240	22	22	0.260	23	23	0.060	24	24	0.080
<u>F_B</u>											
1	7	0.389	2	7	0.365	8	4	0.187	8	7	0.019
8	17	-0.090	8	18	-0.090	9	5	0.130	9	7	0.181
9	17	-0.090	9	19	-0.090	10	6	0.393	10	7	0.393
10	18	-0.090	10	19	-0.090	11	7	0.281	12	7	0.308

*Only nonzero elements are listed. The numbering of the internal coordinates is in accordance with the order in which they are listed in the text.(p.78).

For F_A, which is symmetric, only elements on the main diagonal and above it are listed.

The vibrational frequencies were calculated by solving the secular equation (2.20) of dimensions 24×24 for values of the phase difference δ ranging from 0 to π in steps of 0.1π . The dispersion curves were thus obtained.

Experimental

For the extended chain structure, the A species vibrations, which correspond to the phase difference $\delta = 0$, and the B species vibrations, which correspond to $\delta = 5\pi/9$ are infrared active. The calculated values of the optically active frequencies were fitted by comparison with observed infrared frequencies. Attempts to prepare the β -form here from α -polyalanine by solution in dichloroacetic acid or trifluoroacetic acid and stretching in steam resulted only in mixtures of the two forms. In this calculation, therefore, the infrared spectra of β -polyalanine reported by Itoh et al.¹⁰ and information obtained from the work of Elliott¹¹ on the infrared spectra of the β -form above 800 cm^{-1} have been made use of in modifying the force field. The dichroic properties of bands reported by these workers have been of use in making assignments. The infrared spectrum of β -polyalanine is shown in Figure 12.

Discussion

The calculated A frequencies ($\delta = 0$) and B frequencies ($\delta = \pi$) for the β -form of poly-L-alanine are shown, along with the observed infrared frequencies, in Table 12. The potential energy distributions and assignments are also given.

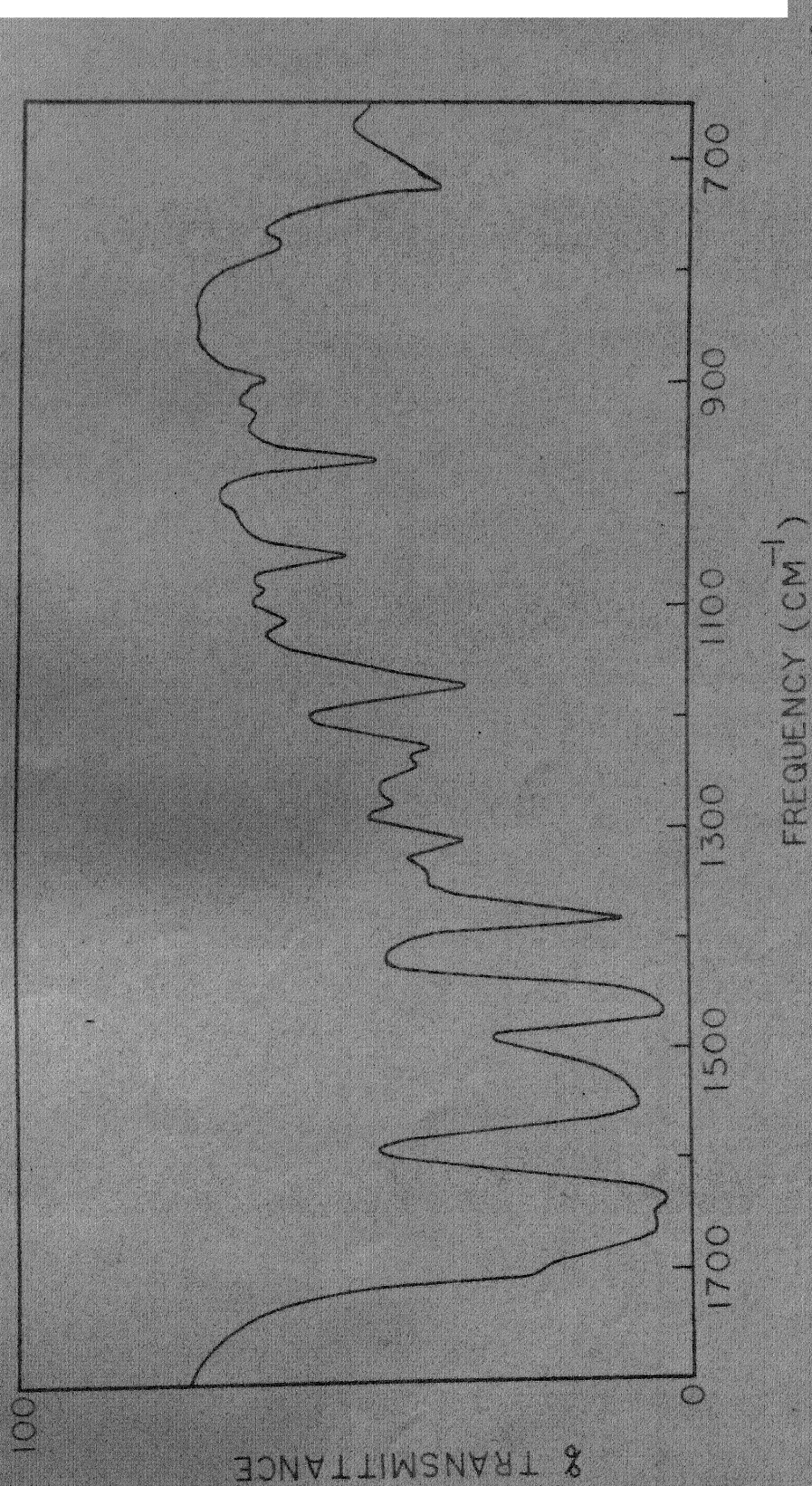


FIG. 12a INFRARED SPECTRUM OF β -POLYALANINE FROM 1800 TO 700 CM⁻¹(10)

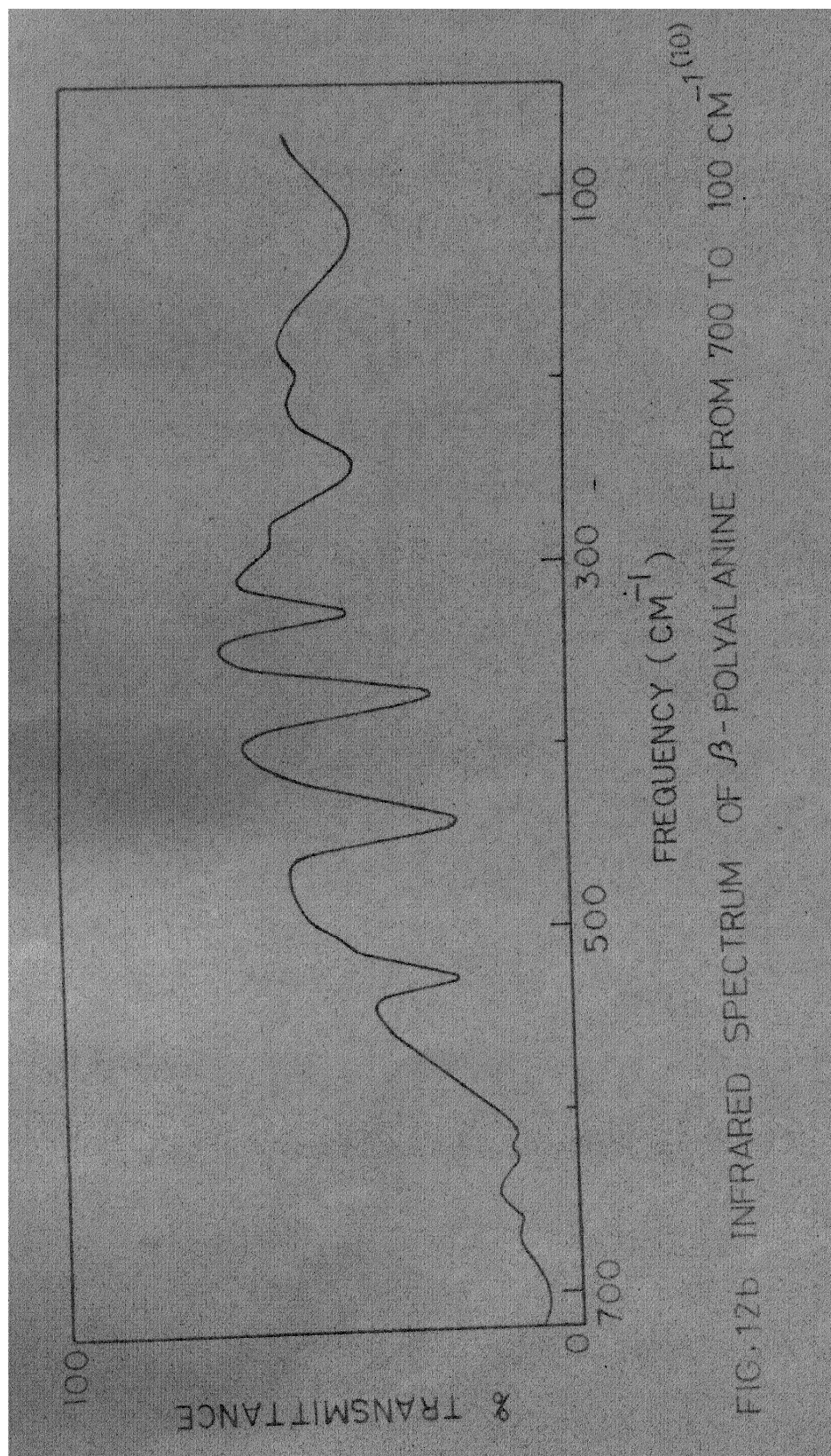


TABLE 12

CALCULATED AND OBSERVED FREQUENCIES FOR β -POLY-L-ALANINEa) A vibrations (phase difference = 0°)^a

Calcu- lated	Observed(ir)	Assignment ^b (P.E.D. (%))
3285	3283	r(N-H) (99)
2912	2883	r(C $_{\alpha}$ -H) (96)
1668	1695	r(C=O) (48), r(C-N) (29) (Amide I).
1530	1524	ϕ (C-N-H)(36), ϕ (H-N-C $_{\alpha}$)(29), r(C-N)(18) (Amide II)
1231	1224	ϕ (H-N-C $_{\alpha}$)(23), ϕ (C-N-H)(16), r(C-N)(12), r(C $_{\alpha}$ -C)(10) (Amide III).
1210	..	ϕ (H-C $_{\alpha}$ -C)(31), ϕ (H-C $_{\alpha}$ -M)(21), ϕ (M-C $_{\alpha}$ -C)(14).
1190	1168	ϕ (M-C $_{\alpha}$ -C)(27), ϕ (N-C $_{\alpha}$ -M)(22), ϕ (H-C $_{\alpha}$ -M)(17), r(C $_{\alpha}$ -M)(8).
1089	1081	r(N-C $_{\alpha}$)(36), r(C-N)(17), ϕ (C-N-C $_{\alpha}$)(16), ϕ (C $_{\alpha}$ -C-N)(9).
1054	..	r(C $_{\alpha}$ -C)(23), r(N-C $_{\alpha}$)(18), ϕ (N-C $_{\alpha}$ -M)(13), r(C-N)(12).
974	967	r(C-N)(29), r(C $_{\alpha}$ -C)(22), ϕ (N-C $_{\alpha}$ -C)(14).
770	771	ϕ (O=C-N)(32), ϕ (C $_{\alpha}$ -C=O)(17), r(C $_{\alpha}$ -M)(15).
631	622	ω (N-H)(31), ω (C=O)(14), ϕ (O=C-N)(11), ϕ (C-N-H) (10) (Amide V).
578	594	ω (C=O)(19), ϕ (O=C-N)(29), ϕ (C $_{\alpha}$ -C=O)(27), ϕ (C $_{\alpha}$ -C-N)(19) (Amide IV, VI).
437	432	ϕ (N-C $_{\alpha}$ -M)(43), ϕ (N-C $_{\alpha}$ -C)(15), ϕ (N-C $_{\alpha}$ -H)(13), t(C-N)(13).
349	..	ϕ (M-C $_{\alpha}$ -C)(28), ϕ (N-C $_{\alpha}$ -M)(17), ϕ (C $_{\alpha}$ -C=O)(9), ϕ (H-C $_{\alpha}$ -M)(9).
238	247	t(C-N)(39), ϕ (N-C $_{\alpha}$ -M)(9), t(N-C $_{\alpha}$)(7), ϕ (N-C $_{\alpha}$ -C)(8) (Amide VII).
202	195	ϕ (C $_{\alpha}$ -C-N)(19), ϕ (C-N-C $_{\alpha}$)(17), ϕ (N-C $_{\alpha}$ -C)(14), ϕ (C $_{\alpha}$ -C=O)(9), ϕ (C-N-H)(7).
151	..	t(N-C $_{\alpha}$)(31), t(C-N)(20), ω (C=O)(11).
65	..	t(C $_{\alpha}$ -C)(27), t(N-C $_{\alpha}$)(21), t(C-N)(18).

Foot-note at the end of the table.

(contd.)

Table 12 (contd.)

b) B vibrations (phase difference = 180°) ^a		
Calcu- lated	Obser- ved(ir)	Assignment ^b (P.E.D. (%))
3285	3283	r(N-H) (99)
2913	2883	r(C _α -H) (95)
1631	1634	r(C=O)(42), r(C-N)(31) (Amide I).
1527	1524	∅(C-N-H)(31), ∅(H-N-C _α)(36), r(C-N)(13) (Amide II).
1259	1241	∅(H-N-C _α)(30), ∅(C-N-H)(24), r(C _α -C)(17). (Amide III).
1237	..	∅(H-C _α -M)(27), ∅(N-C _α -H)(24).
1031	1050	r(C _α -M)(32), ∅(H-C _α -C)(21), ∅(M-C _α -C)(9).
995	1017	r(N-C _α)(27), r(C _α -M)(18), r(C-N)(15).
952	..	r(C _α -C)(29), r(N-C _α)(17), ∅(N-C _α -M)(13), ∅(N-C _α -C)(12).
917	926	r(N-C _α)(32), r(C _α -M)(26), r(C _α -C)(11), ∅(C _α -N-H)(11).
842	..	∅(C _α -C-N)(27), ∅(C _α -C=O)(17), ∅(O=C-N)(14), ∅(M-C _α -C)(11).
730	705	ω(N-H)(51), ω(C=O)(12) (Amide V).
657	657	ω(C=O)(46), ∅(O=C-N)(27), ∅(C _α -C=O)(16) (Amide IV, VI).
554	..	∅(C _α -C-N)(20), ∅(M-C _α -C)(17), ∅(C _α -C=O)(11), ω(C=O)(7), ω(N-H)(7).
406	445	∅(N-C _α -M)(30), ∅(N-C _α -C)(17), ∅(N-C _α -H)(10), t(C-N)(9).
298	..	t(C-N)(37), t(N-C _α)(14), ∅(N-C _α -C)(11) (Amide VII).
282	..	∅(O=C-N)(21), ∅(C _α -C=O)(15), ∅(M-C _α -C)(15), ∅(N-C _α -C)(12).
123	122	t(C _o -C)(34), t(C-N)(20).
88	..	t(N-C _α)(41), t(C _α -C)(22), t(C-N)(12).

^a All frequencies are in cm⁻¹.

^b r: bond stretching; ∅: in-plane angle bend; ω: out-of-peptide-plane angle bend. Only major contributions to the P.E.D. are listed.

As already pointed out, the optically active frequencies in the far-infrared region are of particular interest in connection with conformation studies. The Amide V band for β -poly-alanine is observed at 705 cm^{-1} ¹². This corresponds to the B mode calculated at 730 cm^{-1} . The A end of this mode is calculated at 631 cm^{-1} and corresponds to the observed band at 622 cm^{-1} . The bands at 594 and 657 cm^{-1} are associated with the Amide IV and VI vibrations. The 594 cm^{-1} band corresponds to the calculated mode at 578 cm^{-1} . It is essentially due to the $\text{O}=\text{C}-\text{N}$ in-plane bending, but has a small amount of $\text{C}=\text{O}$ wag. The B end of this mode is calculated at 657 cm^{-1} , and has a large percentage of the $\text{C}=\text{O}$ wag. It is, therefore, identified with the Amide VI band.

As has been already mentioned, the Amide VII band arising out of torsional motion around the peptide $\text{C}-\text{N}$ bond could be of use in conformation diagnoses. The broad parallel band at 247 cm^{-1} is assigned to this torsional mode¹⁰. This corresponds to the calculated A frequency of 238 cm^{-1} . The A end of the Amide VII frequency in polyglycine I,⁹ which has a similar structure, is at 231 cm^{-1} . The B end of this mode in poly-L-alanine is calculated at 298 cm^{-1} . In addition to this torsional mode, there are two other skeletal modes in the frequency region below 200 cm^{-1} . These modes involve mixtures of torsions around the $\text{C}-\text{N}$, $\text{C}-\text{C}_\alpha$ and $\text{N}-\text{C}_\alpha$ bonds along the chain. While the calculation for the β -form shows two such modes, the α -form has one such low-lying torsional mode.

The dispersion curves for the β -form of poly-L-alanine are shown in Figure 13. Modes with higher frequencies, which do not show appreciable dispersion, have not been included. Since the model of the polymer used is an isolated chain, there exist four zero frequencies, that is, four acoustic modes. These four frequencies correspond to translations along three perpendicular directions and rotation about the axis of the chain. At $\delta = 0$, the two acoustic branches correspond to the translational mode along the chain axis and rotational mode about the axis. At $\delta = \pi$, they correspond to the translational modes perpendicular to the axis.

It is of interest to note that the dispersion curves for the β -form do not show a tendency to crowd closer together near the $\delta = \pi$ end as do the curves for the α -helix. This feature is also true of the dispersion curves of polyethylene¹³, which takes the planar zig-zag configuration, and those of polyglycine I⁹, which is in an extended configuration. In fact, in the former, the curves come close together at the $\delta = 0$ end, and fan out, appearing to repel each other towards the zone boundary. This common feature is no doubt due to the absence of strong intrachain interactions stabilising the structure, in contrast to the case of the hydrogen-bonded α -helix.

The dispersion curves for the amide V, VII vibrations are of special interest in connection with conformation. The

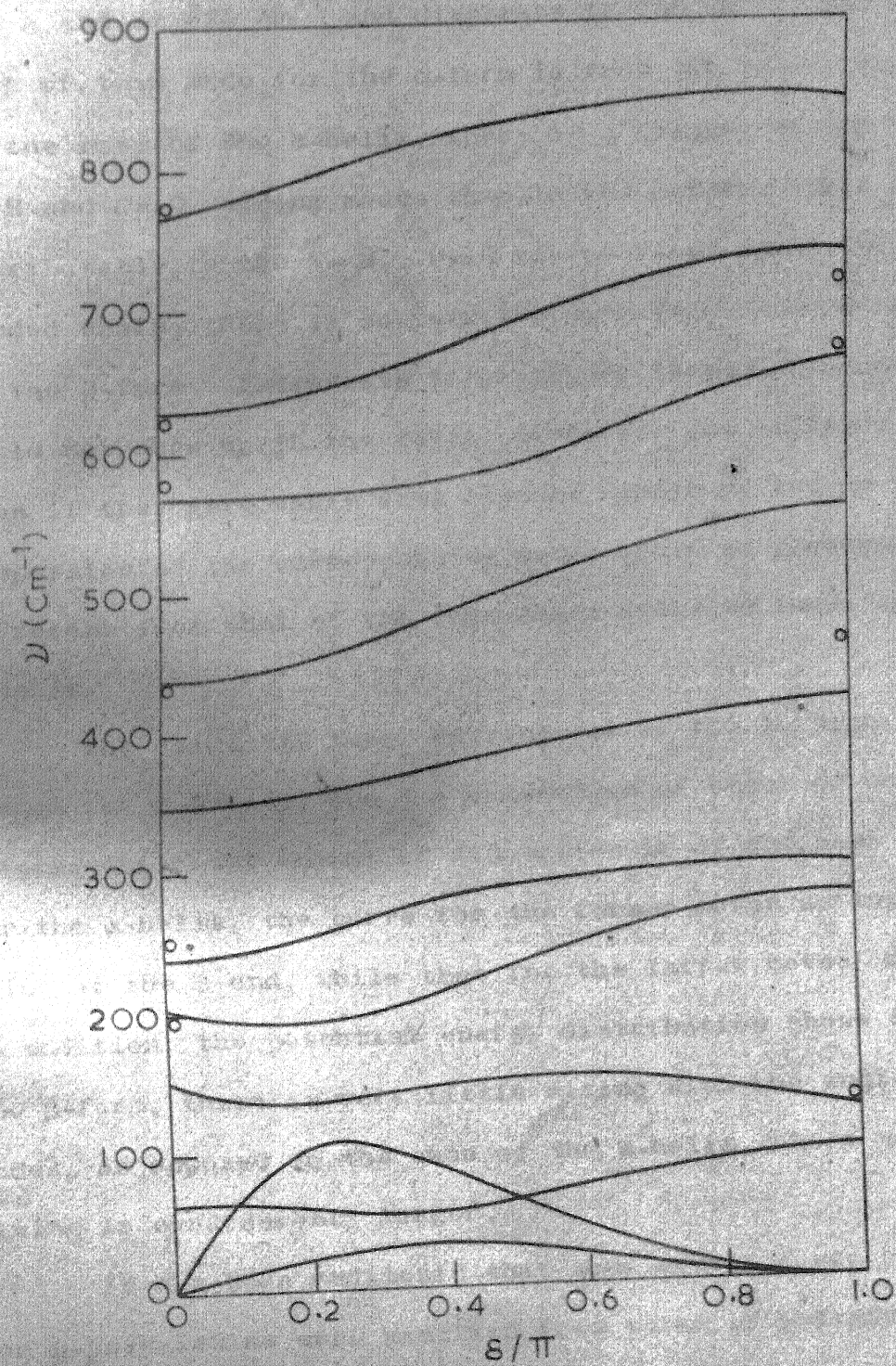


FIG. 13 DISPERSION CURVES FOR β POLY-L-ALANINE

its A end at 622 cm^{-1} , and disperses to 730 cm^{-1} . The dispersion of this mode for the α -form is from 581 to 618 cm^{-1} .

In the case of the α -helix, there is a greater mixing of the N-H and C=O wagging modes than in the β -form. This is attributable to the N-H...O=C interactions along the hydrogen bonded chain; there is no corresponding intrachain interaction in the β -form. Interchain interactions through hydrogen bonds would not show up in the calculations for the isolated chain; even if they were taken into account, their effect on the dispersion of the corresponding modes would be presumably different from that of the intrachain hydrogen bonds in the α -helix.

The amide VII band, arising out of the torsional motion around the C-N bond, shows a dispersion of about 60 cm^{-1} in the β -form; while the amount of dispersion is of the same order for the α -helix, the curve for the former moves 'up' towards its value at the B end, while that for the latter moves 'down'. In addition, the potential energy distribution shows that for the β -form, there is very little mixing with the angle-bending modes, as opposed to the case of the α -helix, where such mixing is considerably larger.

It has been mentioned that some of the force constants for β -polyalanine were modified from those of polyglycine I⁹. This is because, in spite of the similarity in the two structures, the presence of the heavy methyl groups would modify interactions involving the α -carbon atom. On the other

and, the helical forms of these polypeptides differ appreciably in their structures (polyglycine II is a 3-fold helix, without intrachain hydrogen bonds, while poly-L-alanine exists as an α -helix stabilised by intrachain hydrogen bonds) and hence the force fields would be expected to be quite different for the two helices. Comparison with calculations on the polyglycine II helix¹⁴ shows that this is the case.

In conclusion, it must be remarked that the isolated chain is a very much simplified model when one considers the actual conditions prevailing in a crystal. This is especially true for the β -form of poly-L-alanine, where interchain hydrogen bonds play an important part in stabilising the structure. The effects that would be expected if one considers a three-dimensional model are discussed in detail in the next chapter; however, the dispersion curve calculations for an isolated chain can serve as a useful starting point and provide certain interesting results on the nature of the vibrational modes.

REFERENCES

1. L. Pauling and R.B. Corey, Proc. Natl. Acad. Sci. 37, 235 (1951).
2. L. Pauling and R.B. Corey, Proc. Natl. Acad. Sci. 37, 729 (1951).
3. L. Pauling and R.B. Corey, Proc. Natl. Acad. Sci. 39, 253 (1953).
4. C.H. Bamford, L. Brown, A. Elliott, W.E. Hanby, and I.F. Trotter, Nature 173, 27 (1954).
5. L. Brown and I.F. Trotter, Trans. Faraday Soc. 52, 537 (1956).
6. S. Arnott, S.D. Dover, and A. Elliott, J. Mol. Biol. 30, 201 (1967).
7. R.B. Corey and L. Pauling, Proc. Roy. Soc. (London) B141, 10 (1953).
8. T. Miyazawa, private communication.
9. V.D. Gupta, S. Trevino, and H. Boutin, J. Chem. Phys. 48, 3008 (1968).
10. K. Itoh, T. Nakahara, T. Shimanouchi, M. Oya, K. Uno, and Y. Iwakura, Biopolymers 6, 1759 (1968).
11. A. Elliott, Proc. Roy. Soc. (London) A226, 408 (1954).
12. Y. Masuda, K. Fukushima, T. Fujii, and T. Miyazawa, Biopolymers 8, 91 (1969).
13. L. Piseri and G. Zerbi, J. Chem. Phys. 48, 3561 (1968).
14. R.D. Singh and V.D. Gupta, Spectrochim. Acta (in press).

CHAPTER VI

CONCLUSION

In the preceding pages, the problem of the vibrations of the polyalanine chain has been studied by regarding the polypeptide as an isolated, infinite, single chain. It is clear that the physical state of affairs in a real crystal is quite different from the simplified model. A fuller interpretation of the vibrational modes would require calculations on a three-dimensional system, taking into account intermolecular interactions. In principle, the vibrational problem of a three-dimensional system can be treated in an analogous way; however, the calculations become extremely cumbersome, and the matrices which have to be handled are of inconvenient dimensions.

The general effects on the frequency spectrum to be expected as a result of intermolecular interactions in a crystal can be fairly easily visualised¹. The ordered crystalline forces will, in the first place, produce slight shifts in the frequencies from those calculated for the free molecule. When considering a three-dimensional system, one has to take into account the symmetry and contents of a unit cell. The former is in general lower than that of the free molecule. This lowering of the symmetry of the molecular environment, together with the mechanical coupling with neighbouring chains, will result in a multiplication in the number of optically active frequencies. In addition, low-frequency lattice modes will

appear in the vibrational spectrum. Since these lattice motions are highly concentrated in a narrow frequency range below 200 cm^{-1} , the densities of vibrational states will be strongly modified in the lower frequency region in going from a single chain model to a three-dimensional one. These effects can be studied in a quantitative manner only when the nature of the intermolecular interactions is more accurately known.

Calculations of phonon dispersion curves of three-dimensional crystalline polymer systems have been made only for the simpler polymers, such as polyethylene², which possesses a relatively simple molecular and crystal structure. These calculations have provided values for the intermolecular forces in the harmonic approximation. Relatively little is known about these forces for helical polymers. The observed vibrational spectra of most polymeric systems have so far been sought to be interpreted in terms of the single chain model. Coming to the case of the polypeptides, Fukushima and Miyazawa³ have taken into account the interchain force field associated with the stretching and bending modes of the $\text{N-H}\cdots\text{O}=\text{C}$ hydrogen bonds and treated the vibrations of crystalline polyglycine I in the antiparallel chain pleated-sheet structure. Complete calculations on a three-dimensional crystal of polyalanine would have to take into account, in addition to interactions through the intermolecular hydrogen bonds, also the influence of the methyl groups, whose steric hindrance plays a large role in the packing of chains in the lattice,

both in the α - and β -forms. Moreover, as mentioned earlier, the fact that poly-L-alanine in the β -form can be described only in terms of a statistical unit cell⁴, would introduce complications in calculations for a three-dimensional system.

Assuming this admittedly simplified model for the poly-L-alanine chain, it has, nevertheless, been possible to find reasonable correlation with observed spectra and to obtain conclusions which may be of use in relation with conformation studies. In particular, the dispersion of the N-H out-of-plane wagging mode (amide V) and the C-N torsional mode (amide VII) in the two forms could be of help in further elucidating the nature of these modes in the context of conformational differences. The difference in the dispersion of the amide V mode for the two cases has been pointed out; it is certainly related to the effect of hydrogen bonding. While for the α -helix hydrogen bonding is intrachain, the hydrogen bonding is interchain in the β -form. Although interactions through hydrogen bonds have not been explicitly considered for the β -form, the adjustment of force constants to obtain agreement with observed frequencies has effectively taken into account these interactions in a circuitous manner. The relative strengths of the hydrogen bonds in the two cases would be expected to influence the nature of the dispersion of the modes.

Coming to the C-N torsional mode, the calculation has shown that the frequencies for the two forms at the A end

are not appreciably different, but at the E end they differ by as much as 110 cm^{-1} . In other words, the nature of dispersion of the mode in the two cases is vastly different. In the case of polyglycine, the A end frequencies for the two forms I and II are far apart, namely, at 217 cm^{-1} and 365 cm^{-1} respectively⁵. Now, the β -form of poly-L-alanine and polyglycine I have similar structures. The dispersion of the peptide C-N torsional mode in the two cases does follow similar lines. However, polyglycine II exists as a 3-fold helix; unlike the α -helix of poly-L-alanine, it does not have intrachain hydrogen bonds. The dispersion of the torsional mode in the two cases is different. While in α -polyalanine the dispersion is from 230 to 184 cm^{-1} , in polyglycine II⁶, the mode disperses from 360 to above 400 cm^{-1} . It thus seems likely that this torsional deformation mode of the chain is also dependent on the nature of $\text{N-H}\cdots\text{O}=\text{C}$ hydrogen bonding in the structure - whether it is interchain or intrachain. Further, since the torsional mode involves large amplitudes of the α -carbon atom, the nature of the side groups and their vibrations should influence, to a certain extent, the dispersion of the mode. The light hydrogen atom of polyglycine is replaced by the heavy methyl group in polyalanine, which would damp the motion of the α -carbon atom. Thus calculations considering the four atoms of the methyl group separately instead of as a single unit would help in elucidating the nature and extent of the interaction of side chain modes with skeletal vibrations. A systematic study of

polypeptides with successively larger alkyl side groups is necessary in order to obtain further useful information regarding the correlations between the torsional modes and conformation. The calculations for poly-L-alanine, it is hoped, may serve as a starting point.

The use of dispersion curves in calculating thermodynamic quantities has been mentioned. Several thermodynamic parameters such as internal energy, specific heat and entropy are dependent on the frequency distribution functions, which, in turn, can be obtained from the dispersion relations. In particular, the specific heat is known to be sensitive to the low-frequency modes, arising mostly out of the skeletal and torsional vibrations. A knowledge of the dispersion of these modes would allow specific heat calculations to be made for different conformations, and help in studying the dependence of specific heat on conformation of polypeptide systems.

REFERENCES

1. G. Zerbi, Appl. Spectroscopy Reviews 2, 193 (1969).
2. S. Enomoto and M. Asahina, J. Polymer Sci. A2, 3523 (1964);
M. Tasumi and T. Shimanouchi, J. Chem. Phys. 43, 1245 (1965);
M. Tasumi and S. Krimm, J. Chem. Phys. 46, 755 (1967).
3. T. Miyazawa, in "Poly- α -amino acids", G.D. Fasman, Ed.,
Marcel Dekker, Inc., New York, 1967, Chapter 2.
4. S. Arnott, S.D. Dover, and A. Elliott, J. Mol. Biol. 30,
201 (1967).
5. T. Miyazawa, Bull. Chem. Soc. Japan 34, 691 (1961).
6. R.D. Singh and V.D. Gupta, Spectrochim. Acta (in press).

SOME OF THE WORK DESCRIBED IN THIS
THESIS HAS BEEN PUBLISHED. A LIST
OF REFERENCES APPEARS BELOW:

1. V.D. Gupta and M.V. Krishnan, 'Low-frequency spectra of L-alanine', J. Phys. B 3, 572 (1970).
2. M.V. Krishnan and V.D. Gupta, 'Vibration spectra of α -helix of polyalanine', Chem. Phys. Letters 6, 231 (1970).
3. V.D. Gupta, A.K. Gupta, and M.V. Krishnan, 'Vibrational properties of polyglycine chain', Chem. Phys. Letters (accepted for publication).
4. M.V. Krishnan and V.D. Gupta, 'Dispersion curves of polyalanine in the β -form', Chem. Phys. Letters (accepted for publication).

